European Journal of Inorganic Chemistry

Syntheses, Crystal Structures and Magnetic Properties of a Series of Defect-Dicubane Tetranickel(II) Systems with Variable, Mixed and Interchangeable μ3-Core Ligands

--Manuscript Draft--

Manuscript Number:	ejic.201900649R3
Article Type:	Full Paper
Corresponding Author:	Sasankasekhar Mohanta University of Calcutta Kolkata, INDIA
Corresponding Author E-Mail:	sm_cu_chem@yahoo.co.in
Order of Authors (with Contributor Roles):	Shuvayan Roy
	Hazel A. Sparkes
	Sasankasekhar Mohanta
Keywords:	Magnetic Properties / Tetranickel(II) / Defect Dicubane / Ferromagnetic / Heterobridged
Abstract:	The article describes syntheses, crystal structures and magnetic properties of six defective dicubane type NiII4 clusters of compositions [NiII4(HL1)2(μ3-X)2(μ1,1-N3)2(μ1,3-carboxylato)2]·nH2O (1, X = OMe–, carboxylato = o-benzoylbenzoato, n = 0; 2, X = {(OMe–)0.83(N3–)0.17}, carboxylato = phenyl acetato, n = 2; 3, X = {(OMe–)0.80(N3–)0.20}, carboxylato = salicylato, n = 0; 4, X = OH–, carboxylato = o-benzoylbenzoato, n = 2; 5, X = {(N3–)0.58(OMe–)0.42}, carboxylato = o-benzoylbenzoato, n = 2) and [NiII4(HL1)2(μ1,1,1-N3)2(μ1,1-N3)2(N3)2(H2O)2]·4DMF (6), where H2L1 is 2-Formyl-6-{(2-hydroxy-1,1-dimethyl-ethylimino)-methyl}-4-ethyl-phenol, and this is the partially hydrolysed product of initially employed ligand H3L, 2,6-Bis-{(2-hydroxy-1,1-dimethyl-ethylimino)-methyl}-4-ethyl-phenol. Each of the two compartments of each [HL1]– in 1–6 is occupied by a NiII ion, to form a NiII2 fragment. The common bridges between the two metal ions in a dinuclear fragment are μ-phenoxo of [HL1]– and one μ3-core ligand (methoxo/hydroxo/mixture of methoxo and μ1,1,1-azido) while the additional bridge in 1–5 is a μ1,3-carboxylato. Two dinuclear fragments are interlinked by two μ1,1-azido and two μ3-core ligands. Interestingly, the μ3-methoxo compound 1 and the μ3-hydroxo compound 4 are interconvertible in both ways as the function of the solvents. Variable-temperature and variable-field magnetic studies reveal overall ferromagnetic interactions in each of 1–6.
Response to Reviewers:	Response to Editor's Comments Manuscript number: ejic.201900649R2 MS Type: Full Paper Title: "Syntheses, Crystal Structures and Magnetic Properties of a Series of Defect-Dicubane Tetranickel(II) Systems with Variable, Mixed and Interchangeable μ3-Core Ligands" Correspondence Author: Prof. Sasankasekhar Mohanta Final version due: 18th October 2019 1.File format: Please provide the final revision as a Microsoft Word file that can be used for production. Authors' Response: Done as suggested. 2. Graphic Upload: To ensure the best possible quality of your final article, we require the original graphic files for all schemes, figures, and formulae as well as the graphical abstract in high resolution (300 dpi in general and 600 dpi for bitmap graphics). Please upload all graphic files. Acceptable formats are .tif, .jpeg, .gif, or .png files; ChemDraw structures should be uploaded as .cdx files. You may upload all files compressed in a ZIP archive. Authors' Response:

	Done as suggested. Please see the zip file named Figures-zip. 3. Supporting Information: All ok, please upload again as is. Authors' Response: Done as suggested. 4. Address: Information is missing or incomplete: - Academic titles are missing: Please provide the names and academic titles (e.g., Prof., Dr., or Prof. Dr.) for all authors in the address block. Authors' Response: revised as suggested. - Twitter: Should you or your institute have a Twitter account, please let us know the appropriate username. All our content is automatically shared on Twitter once the final version of the article gets published online. Our editors write the Tweets and are happy to add your accounts. Please note that you will be able to make corrections in your galley proof. Authors' Response: We have no such Twitter. 5. Multiple Graphic Files: We noticed that some of your graphics contain several parts (see schemes 1 - 4 and Figs 1, 2 and 5). Please make sure to combine them into just one graphic file and upload one file per graphic. Authors' Response: Done as suggested. 6. Missing Cross-Reference: During the typesetting process, graphics and tables are attached after the paragraph where they are first mentioned. Please mention each graphic and table in the paragraph under which you wish them to appear. In your manuscript, Figure 6 is not mentioned in the text. Please check and correct. Authors' Response: There are five Figures: Figure 1 – Figure 5. So query about Figure 6 does not arise. 7. Please remove "Angew. Chem. Int. Ed." from reference 8e. Authors' Response: Revised as suggested.
Section/Category:	
Additional Information:	
Question	**Response**
Submitted solely to this journal?	Yes
Has there been a previous version?	No
Do you or any of your co-authors have a conflict of interest to declare?	No
Does the research described in this manuscript include animal experiments or human subjects or tissue samples from human subjects?	No

Syntheses, Crystal Structures and Magnetic Properties of a Series of Defect-Dicubane Tetranickel(II) Systems with Variable, Mixed and Interchangeable μ_3-Core Ligands

Shuvayan Roy,[a] Hazel A. Sparkes[b] and Sasankasekhar Mohanta*[a]

[a] *S. Roy and Prof. S. Mohanta*
Department of Chemistry, Inorganic Chemistry Section, University of Calcutta
92 A. P. C Road, Kolkata 700 009, India
E-mail: sm_cu_chem@yahoo.co.in.
Fax: 91-33-23519755
http://www.caluniv.ac.in/academic/department/Chemistry/Sasankasekhar-Mohanta.pdf

[b] *Dr. H. A. Sparkes*
School of Chemistry, University of Bristol, Cantock's Close, Bristol, BS8 1TS, UK.

Supporting information and ORCID(s) from the author(s) for this article are available on the WWW under https://doi.org/10.1002/ejic.201900649.

The article describes syntheses, crystal structures and magnetic properties of six defective dicubane type Ni^{II}_4 clusters of compositions $[Ni^{II}_4(HL^1)_2(\mu_3\text{-}X)_2(\mu_{1,1}\text{-}N_3)_2(\mu_{1,3}\text{-carboxylato})_2]\cdot n H_2O$ (**1**, X = OMe^-, carboxylato = *o*-benzoylbenzoato, *n* = 0; **2**, X = $\{(OMe^-)_{0.83}(N_3^-)_{0.17}\}$, carboxylato = phenyl acetato, *n* = 2; **3**, X = $\{(OMe^-)_{0.80}(N_3^-)_{0.20}\}$, carboxylato = salicylato, *n* = 0; **4**, X = OH^-, carboxylato = *o*-benzoylbenzoato, *n* = 2; **5**, X = $\{(N_3^-)_{0.58}(OMe^-)_{0.42}\}$, carboxylato = *o*-benzoylbenzoato, *n* = 2) and $[Ni^{II}_4(HL^1)_2(\mu_{1,1,1}\text{-}N_3)_2(\mu_{1,1}\text{-}N_3)_2(N_3)_2(H_2O)_2]\cdot 4DMF$ (**6**), where H_2L^1 is 2-Formyl-6-{(2-hydroxy-1,1-dimethyl-ethylimino)-methyl}-4-ethyl-phenol, and this is the partially hydrolysed product of initially employed ligand H_3L, 2,6-Bis-{(2-hydroxy-1,1-dimethyl-ethylimino)-methyl}-4-ethyl-phenol. Each of the two compartments of each $[HL^1]^-$ in **1**–**6** is occupied by a Ni^{II} ion, to form a Ni^{II}_2 fragment. The common bridges between the two metal ions in a dinuclear fragment are μ-phenoxo of $[HL^1]^-$ and one μ_3-core ligand (methoxo/hydroxo/mixture of methoxo and $\mu_{1,1,1}$-azido) while the additional bridge in **1**–**5** is a $\mu_{1,3}$-carboxylato. Two dinuclear fragments are interlinked by two $\mu_{1,1}$-azido and two μ_3-core ligands. Interestingly, the μ_3-methoxo compound **1** and the μ_3-hydroxo compound **4** are interconvertible in both ways as the function of the solvents. Variable-temperature and variable-field magnetic studies reveal overall ferromagnetic interactions in each of **1**–**6**.

Introduction

Molecular magnetism has been a frontier level research area over the last few decades. The key foci of molecular magnetism are the following: (i) Understanding of the intimate relationship of spin coupling[1] from the analyses of the concerned orbitals; (ii) Determination of both experimental and theoretical magneto-structural correlations[2] in simple systems; (iii) Application of the correlations in complex systems that have several exchange pathways to explain or assign their magnetic interactions to appropriate routes;[3–6] (iv) Development of magnetic materials[7–9] including single molecule magnets (SMMs)[8] and single ion magnets (SIMs).[9]

Isolation of new polynuclear clusters is a fascinating as well as challenging aspect in the broad area of inorganic chemistry and coordination chemistry. For tetrametallic clusters,

one familiar motif is defect-dicubane. It may be mentioned that there are a number of defect-dicubane compounds having only 3d metal ions,[3b–g,4–6,10] only 4f metal ions[8e] and both 3d and 4f metal ions.[11]

The choice or design of ligands and self-assembling[3h,i] are crucial for stabilizing clusters[3–6,8,10,11] (as well as coordination polymers, CPs[7,12]). The symmetric two-compartmental Schiff base ligands (like H_3L; two O(alcohol)N(imine)O(phenol) sites; Scheme 1) that are obtained from [1+2] condensation of a 4-R-2,6-diformylphenol (R = Me, Et, *n*-butyl, *tert*-butyl, Cl, CF_3, etc.) and an aminoalcohol or aminophenol is a good member for stabilizing clusters or CPs because of the presence of three possible bridging sites (two alkoxido and one phenoxo) in their deprotonated forms. The possibility of getting clusters and CPs gets obviously enhanced when other potential bridging ligands like azido or a carboxylato or both are also used along with H_3L type ligands. In fact, a number of clusters and some CPs produced on following this approach are known[5,6,13] and some of those compounds are defect-dicubane Ni^{II}_4 systems as well.[5,6] In some rare cases, partial hydrolysis of H_3L type symmetric ligand takes place during the course of the formation of the metal complexes and therefore the final compound contains deprotonated forms of unsymmetrical Schiff base ligands (like H_2L^1; one O(alcohol)N(imine)O(phenol) site and one O(aldehyde)O(phenol) site; Scheme 1).[4,13a] It may be mentioned that one defect-dicubane Ni^{II}_4 complex contains such partially hydrolyzed ligand system.[4]

Our aim of this investigation has been the syntheses, characterization and magnetic studies of a series of Ni^{II} compounds using the new Schiff base ligand, H_3L (Scheme 1; 1:2 condensation product of 4-ethyl-2,6-diformylphenol and 2-amino-2-methyl-1-propanol) as the base ligand and also using azido and various carboxylatos as the secondary bridging ligands. During the formation of complexes, partial hydrolysis of H_3L takes place and six defect-dicubane Ni^{II}_4 compounds of the following compositions have been isolated (H_2L^1 is shown in Scheme 1): $[Ni^{II}_4(HL^1)_2(\mu_3\text{-}X)_2(\mu_{1,1}\text{-}N_3)_2(\mu_{1,3}\text{-carboxylato})_2]\cdot n H_2O$ (**1**, X = OMe^-, carboxylato = *o*-benzoylbenzoato, *n* = 0; **2**, X = $\{(OMe^-)_{0.83}(N_3^-)_{0.17}\}$, carboxylato = phenyl acetato, *n* = 2; **3**, X = $\{(OMe^-)_{0.80}(N_3^-)_{0.20}\}$, carboxylato = salicylato, *n* = 0; **4**, X = OH^-, carboxylato = *o*-benzoylbenzoato, *n* = 2; **5**, X = $\{(N_3^-)_{0.58}(OMe^-)_{0.42}\}$, carboxylato = *o*-benzoylbenzoato, *n* = 2) and $[Ni^{II}_4(HL^1)_2(\mu_{1,1,1}\text{-}N_3)_2(\mu_{1,1}\text{-}N_3)_2(N_3)_2(H_2O)_2]\cdot 4DMF$ (**6**). Herein, we describe syntheses, chartacterization, crystal structures and magnetic properties of **1**–**6** along with an interesting case of solvent-dependent and both-way interconversion of **1** (having μ_3-methoxo) and **4** (having μ_3-hydroxo).

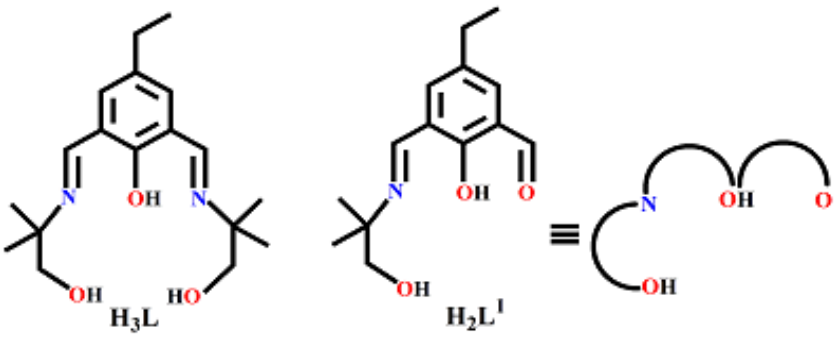

Scheme 1. Chemical structure of the ligands H_3L and H_2L^1.

Results and discussion

Syntheses and FT-IR spectra

The syntheses of the six compounds are illustrated in Scheme 2. Although the symmetrical Schiff base ligand H_3L (Scheme 1; having two O(alcohol)N(imine)O(phenol) compartments) was used in the syntheses of **1**–**6**, they don't contain H_3L or any of its deprotonated forms but they contain a deprotonated form, $[HL^1]^-$, of the unsymmetrical Schiff base ligand H_2L^1 (Scheme 1; having one O(alcohol)N(imine)O(phenol) and one O(aldehyde)O(phenol) compartments). Clearly, partial hydrolysis of H_3L takes place during the formation of the metal complexes **1**–**6**. We were curious to know whether the partial one arm hydrolysis of ligand is metal assisted or not. We have attempted to form *in situ* the H_3L ligand followed by its reaction with copper(II) nitrate, sodium azide and triethyl amine in 1:2:2:3 ratio in H_2O/MeOH medium. This, resulted after few days, green coloured crystalline compounds along with diffractable single crystals of composition $[Cu^{II}_2(H_2L)(\mu_{1,1}\text{-}N_3)(NO_3)(MeOH)]$. Similar type of dinuclear Cu^{II}-based complexes derived from similar type of ligands are reported previously in which two Cu^{II} ions are seated in two O(alcohol)N(imine)O(phenol) compartments of the ligand.[14] Hence, in case of binding with Cu^{II}, *in situ* formed H_3L ligand does not undergo hydrolysis whereas in case of Ni^{II}, partial one arm hydrolysis takes place (Scheme 2). This phenomenon indicates that presence of ligand $[HL^1]^-$ in the crystal structures of **1**–**6**, is due to the Ni^{II} ions present in the reaction medium.

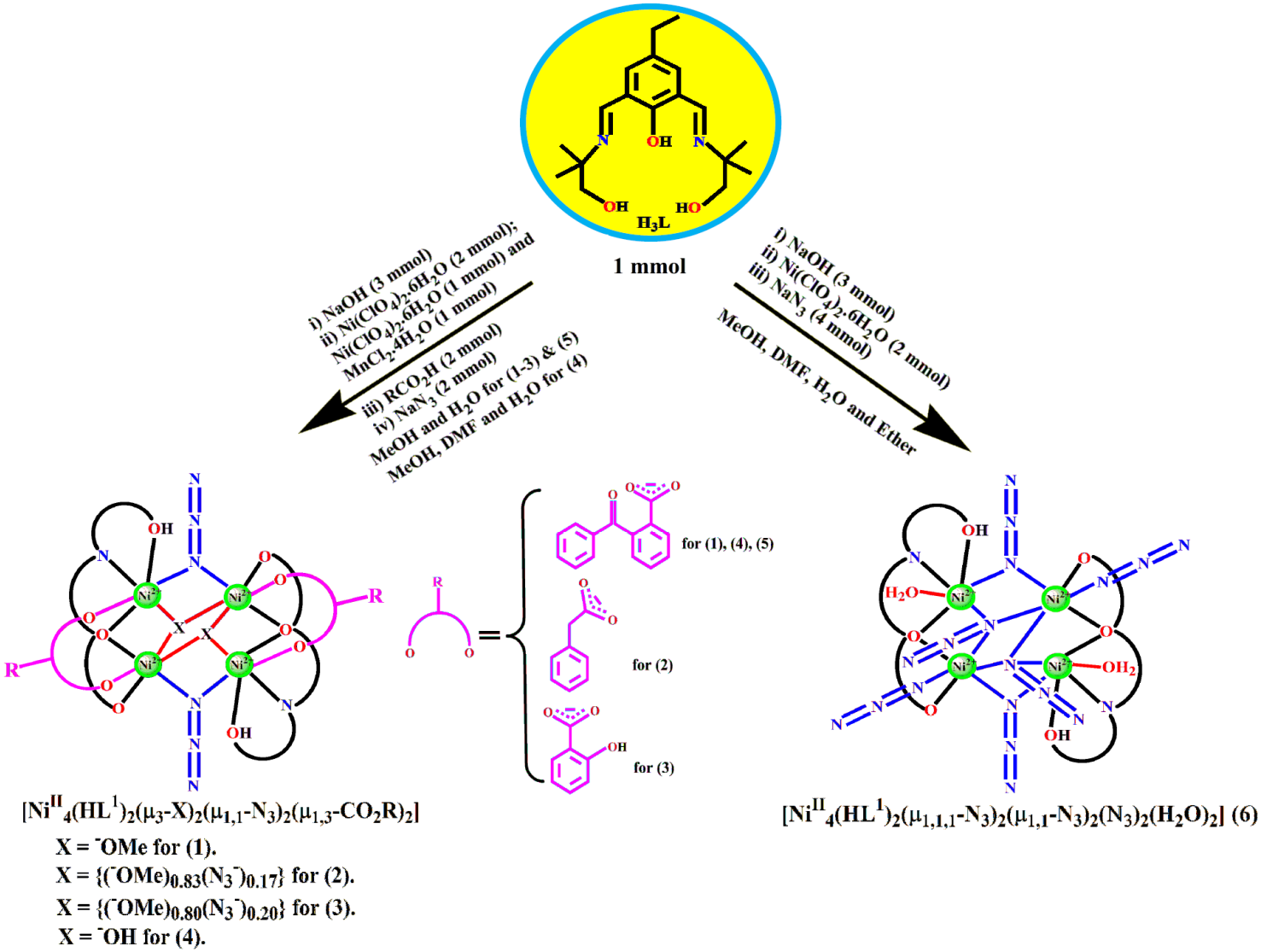

Scheme 2. General schematic illustration of synthetic procedure for all the complexes **1**–**6**.

The tetranuclear compounds **1**–**3**, containing methoxo (for **1**) or 0.83:0.17 (for **2**) and 0.8:0.2 (for **3**) methoxo:$\mu_{1,1,1}$-azido as the μ_3-core ligand and two $\mu_{1,3}$-carboxylatos, were readily prepared on reacting the following reactants in 1:3:2:2:2 ratio: H_3L in methanol, NaOH in water, nickel(II) perchlorate hexahydrate in methanol, a carboxylic acid (*o*-benzoylbenzoic acid, phenyl acetic acid and salicylic acid for **1**–**3**, respectively) in methanol and sodium azide in water (Scheme 2). A similar reaction in which the carboxylic acid is *o*-benzoylbenzoic acid and H_3L (1 mmol) was taken in 15 mL 2:1 methanol-DMF instead of in 10 mL methanol (in **1**–**3**), the compound **4** is produced in which the μ_3-core ligand is hydroxo instead of methoxo or methoxo-azido. The compounds **1** and **4** have the same carboxylato (*o*-benzoylbenzoato) in the tetranuclear cores and have similar strtuctures, except that **1** has a μ_3-methoxo but **4** has a μ_3-hydroxo. Therefore, it seems that the solvents are playing the crucial role in these two compounds in governing the nature of the μ_3-core ligand; **1** is produced in methanol-water, while **4** is produced in methanol-DMF-water, i.e. the presence and absence of DMF is crucial here. To explore this aspect further, we checked whether **4** could be produced from a DMF solution of **1** and **1** could be produced from a methanol solution of **4**. In fact, such reversals occur; the μ_3-hydroxo compound **4** was crystallized when ether was diffused to a DMF solution of the crystalline μ_3-methoxo compound **1** and similarly, the μ_3-methoxo compound **1** was crystallized when ether was diffused to a methanol solution of the crystalline μ_3-hydroxo compound **4** (Scheme 3). Both products in these two conversions were characterized by single crystal X-ray structure determinations. As discussed, Ni^{II}_4 cores in **1**–**5** differ only with respect to the μ_3-core ligand (methoxo/mixture of both methoxo and $\mu_{1,1,1}$-azido/hydroxo), which indicate the stability of such cores and such a stability is better documented by the both-way interconversion between **1** and **4**.

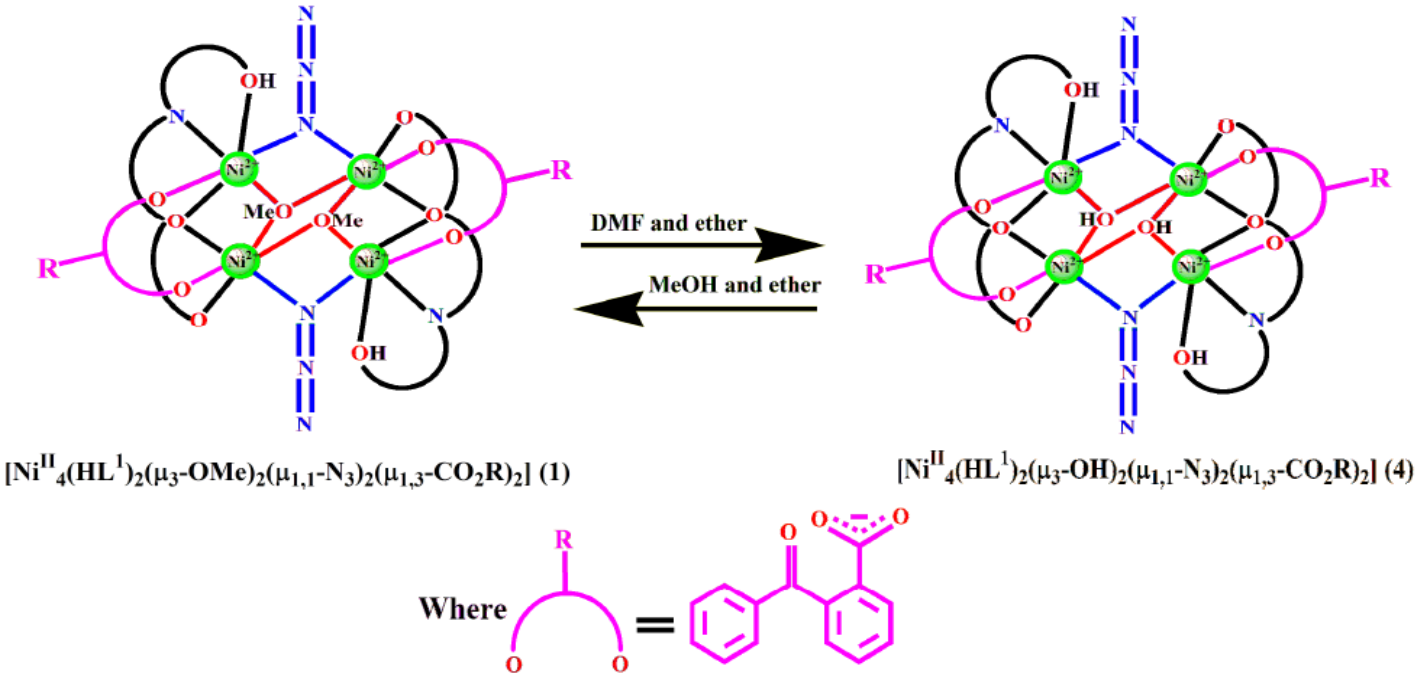

Scheme 3. Schematic representation of solvent-dependent and both-way interconversion between **1** and **4**.

We were attempting to produce heterometallic $Ni^{II}Mn^{II}$ compounds following the similar reactions as mentioned above. On using 1 mmol of $Ni(ClO_4)_2·6H_2O$ and 1 mmol of $MnCl_2·4H_2O$ instead of 2 mmol of $Ni(ClO_4)_2·6H_2O$ in a process similar to that of the preparation of μ_3-methoxo-$\mu_{1,3}$-*o*-benzoylbenzoato compound **1**, we got the $(\mu_{1,1,1}$-azido$)_{0.58}$-$(\mu_3$-methoxo$)_{0.42}$-$\mu_{1,3}$-*o*-benzoylbenzoato compound **5**. If Mn^{II} is not used but even larger amount of azide was used, the product is not **5** but **1**. On the other hand, when *o*-benzoylbenzoic acid was not used and larger amount of azide was utilised, the $\mu_{1,1,1}$-azido compound **6** was produced. This latter compound also contains monodentate azido. All in all, compound **5** was produced in a peculiar way.

FT-IR spectra of all the six compounds were recorded. The compounds **1**–**4** exhibit one band of very strong intensity in the narrow range of 2063–2072 cm^{-1}, which corresponds to one type of azido moiety ($\mu_{1,1}$-); the signal for azido ligand of minor occupancy (in **2** and **3**) does not appear separately. There is a band of very strong intensity at 2063 cm^{-1} and another band of strong intensity at 2092 cm^{-1} in the spectrum of **5**, which correspond to two types of azido ligands ($\mu_{1,1}$- and $\mu_{1,1,1}$-) in it. Three types of azido ligands in **6** are reflected in its FT-IR spectrum as a very strongly intense absorption at 2056 cm^{-1} along with two shoulders (2079 cm^{-1}, strong; 2107 cm^{-1}, weak) appear in the spectrum. Each compound exhibits one absorption of very strong intensity at *ca*. 1650 cm^{-1} and another absorption of strong intensity in the range of 1619–1633 cm^{-1}, which can be assigned to, respectively, aldehyde C=O and imine C=N stretchings. Symmetric and asymmetric stretchings of $\mu_{1,3}$-carboxylato ligands in **1**–**5** appear as bands of medium intensity in the ranges, respectively, 1557–1585 cm^{-1} and 1380–1409 cm^{-1}. The O–H stretchings of water (in **2**, **5** and **6**) or of water and hydroxo (in **4**) appear as a broad band with the center lying in the range of 3416–3451 cm^{-1}.

Description of the crystal structures of 1–6

The crystallographic data for **1**−**6** are summarized in Table S1. All the compounds **1**–**6** crystallize in the same crystal system, monoclinic, but different space group, *C*2/*c* for **1**, $P2_1/c$ for **2**, **4**, **5** and $P2_1/n$ for **3** and **6**, respectively. The structures reveal that the six compounds **1**–**6** are tetranuclear defective dicubane type Ni^{II}_4 systems. The six compounds **1**–**6** can be expressed by the general composition $[Ni^{II}_4(HL^1)_2(\mu_3\text{-X})_2(\mu_{1,1}\text{-}N_3)_2(\mu_{1,3}$-carboxylato$)_2]·n H_2O$ (**1**, X = OMe^-, carboxylato = *o*-benzoylbenzoato, *n* = 0; **2**, X = $\{(OMe^-)_{0.83}(N_3^-)_{0.17}\}$, carboxylato = phenyl acetato, *n* = 2; **3**, X = $\{(OMe^-)_{0.80}(N_3^-)_{0.20}\}$,

carboxylato = salicylato, *n* = 0; **4**, X = OH^-, carboxylato = *o*-benzoylbenzoato, *n* = 2; **5**, X = $\{(N_3^-)_{0.58}(OMe^-)_{0.42}\}$, carboxylato = *o*-benzoylbenzoato, *n* = 2) and $[Ni^{II}_4(HL^1)_2(\mu_{1,1,1}\text{-}N_3)_2(\mu_{1,1}\text{-}N_3)_2(N_3)_2(H_2O)_2]\cdot 4DMF$ (**6**). For all the six compounds, one half is symmetry related to the other half. The tetranuclear cores of **1**–**6** are shown in Figure 1 (for **1** and **4**), 2 (for **5** and **6**) and S1 (for **2** and **3**), respectively, while simplified presentations of the Ni^{II}_4 cores are illustrated in Scheme 2.

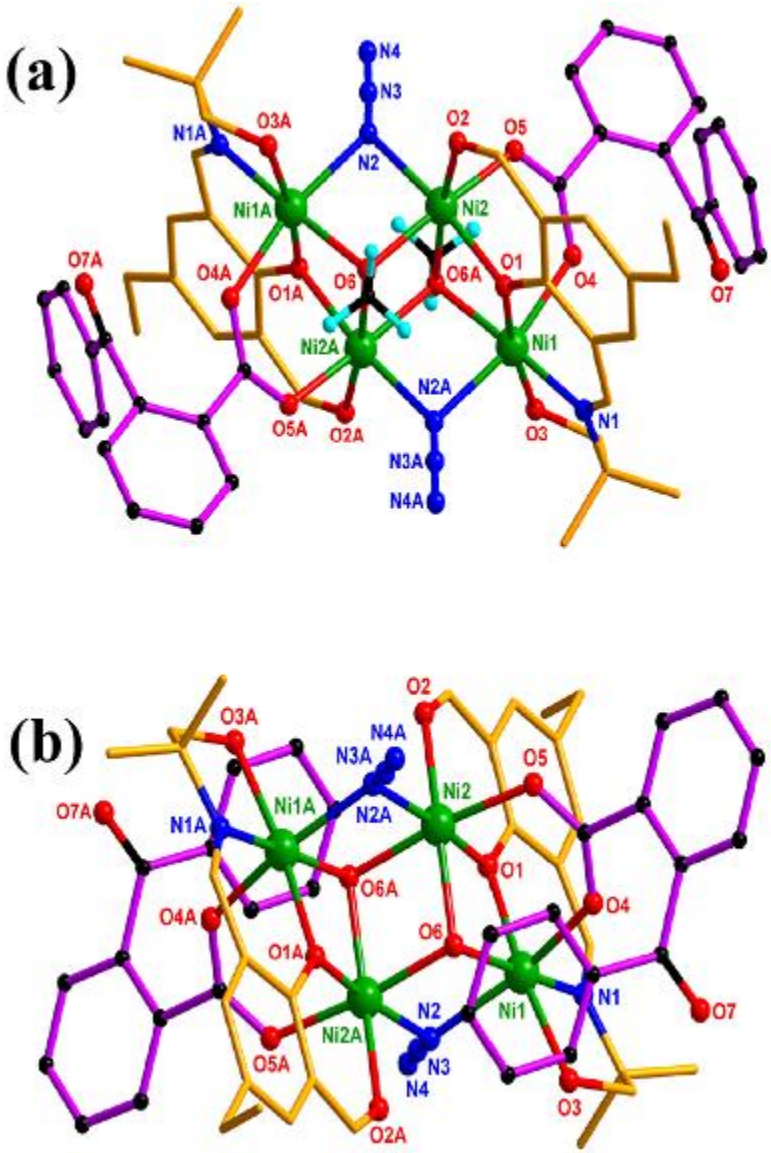

Figure 1. (a) Crystal structure of $[Ni^{II}_4(HL^1)_2(\mu_3\text{-}OMe)_2(\mu_{1,1}\text{-}N_3)_2(\mu_{1,3}\text{-}o\text{-benzoylbenzoato})_2]$ (**1**). All the hydrogen atoms except those of the core μ_3-methoxo bridging ligands have been omitted for clarity. Symmetry code: A = –x, 2–y, 1–z; (b) Crystal structure of $[Ni^{II}_4(HL^1)_2(\mu_3\text{-}OH)_2(\mu_{1,1}\text{-}N_3)_2(\mu_{1,3}\text{-}o\text{-benzoylbenzoato})_2]\cdot 2H_2O$ (**4**). Hydrogen atom on μ_3-hydroxo oxygen atoms (O6/O6A) were not inserted. All the other hydrogen atoms and water molecules of crystallization have been omitted for clarity. Symmetry code: A = 1–x, 1–y, –z.

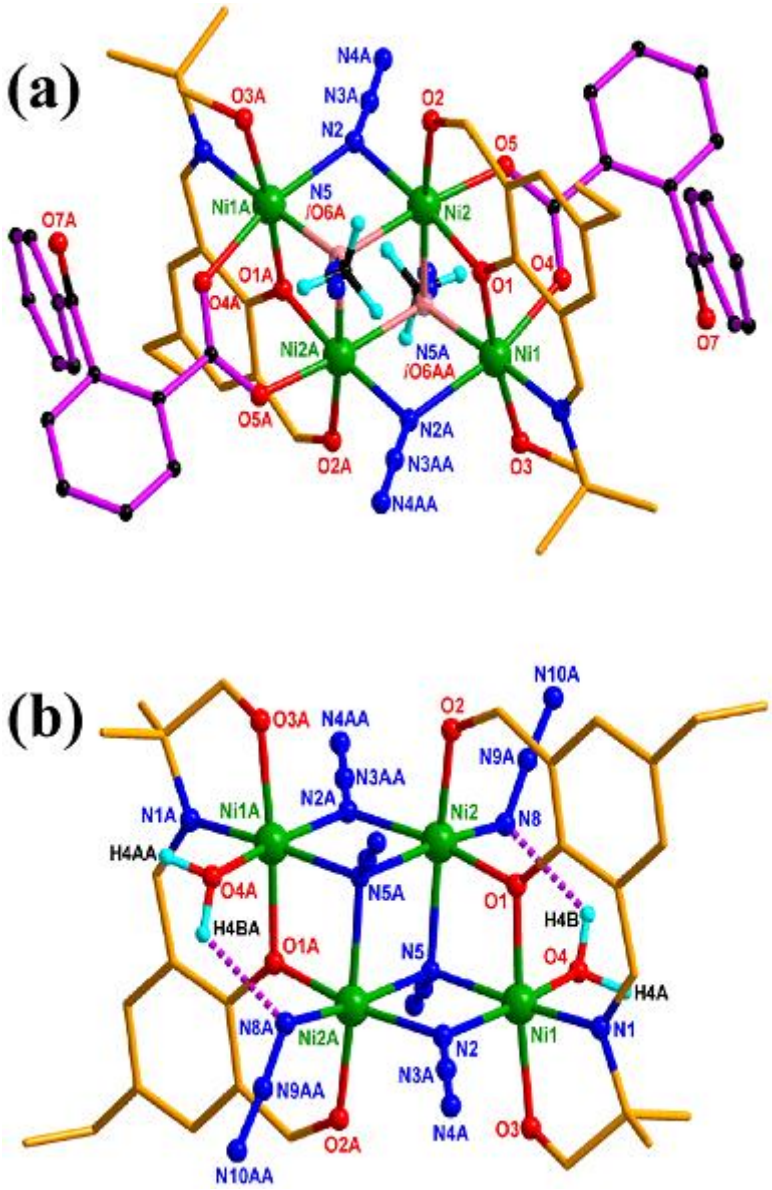

Figure 2. (a) Crystal structure of $[Ni^{II}_4(HL^1)_2\{(\mu_3\text{-}N_3)_{0.58}(\mu_3\text{-}OMe)_{0.42}\}_2(\mu_{1,1}\text{-}N_3)_2(\mu_{1,3}\text{-}o\text{-benzoylbenzoato})_2]\cdot 2H_2O$ (**5**). All the hydrogen atoms except those of the core μ_3-methoxo bridging ligands and two water molecules of crystallisation have been omitted for clarity. Symmetry code: A = 2–x, 1–y, 1–z; (b) Crystal structure of $[Ni^{II}_4(HL^1)_2(\mu_{1,1,1}\text{-}N_3)_2(\mu_{1,1}\text{-}N_3)_2(N_3)_2(OH_2)_2]\cdot 4DMF$ (**6**). All the hydrogen atoms except those of the coordinated water molecules have been omitted for clarity. Four DMF molecules of crystallisation have also been omitted for simplicity. Symmetry code: A = 1–x, 2–y, –z. The dotted lines represent intramolecular hydrogen bonding.

There are a number of general features in the structures of the six Ni^{II}_4 systems **1**–**6**, as mentioned in this paragraph. Each of them contains two Schiff base ligands, $[HL^1]^-$ (Scheme 1), where the phenoxo moiety gets deprotonated. In each compound, each of the two compartments (O(phenoxo)N(imine)O(alcohol) and O(phenoxo)O(aldehyde)) of a $[HL^1]^-$ is occupied by a Ni^{II} ion. Clearly, the phenoxo oxygen atom makes a bridge between the two

Ni^{II} ions accommodated in one $[HL^1]^-$ to generate a monophenoxo-bridged Ni^{II}_2 fragment. Two such symmetry related dinickel(II) fragments are interlinked by four bridging ligands, which are of two of the following types : (i) Peripheral μ-bridging ligands – two $\mu_{1,1}$-azido ligands, each of which bridges one metal ion of one so-called Ni^{II}_2 fragmnent and one metal ion of the second so-called Ni^{II}_2 fragment; (ii) Core μ_3-bridging ligands – two μ_3-methoxo/hydroxo/$\mu_{1,1,1}$-azido or mixture of both μ_3-methoxo/azido ligands, each of which bridges both metal ions of a Ni^{II}_2 fragment and one metal of the second Ni^{II}_2 fragment. The core μ_3-ligand is methoxo for **1**, hydroxo for **4** and $\mu_{1,1,1}$-azido for **6**. In case of **2**, **3** and **5**, it is found that the μ_3-core ligand is a mixture of methoxo and $\mu_{1,1,1}$-azido with incomplete occupancy for each type; 83% methoxo and 17% azido for **2**, 80% methoxo and 20% azido for **3** and 58% azido and 42% methoxo for **5**. Simplified core structures are shown in Figure S2 in which occupancies of the mixed-ligand set in **2**, **3** and **5** are also shown.

As is clear from Figure 1, 2 and S1, the four Ni^{II} ions, μ-phenoxo oxygen atoms, μ_3-hydroxo/methoxo oxygen atoms and the coordinating nitrogen atoms of $\mu_{1,1}$-/$\mu_{1,1,1}$-azido ligands are placed in such a way that a defective dicubane type $Ni_4O_4N_2$ (in **1**−**4**)/$Ni_4O_2N_4$ (**5** and **6**) structure is generated in which the common face is composed of two metal ions (Ni2 and Ni2A) and the coordinating atoms (O6 and O6A or N5 and N5A) of the two core μ_3-bridging ligands.

Another similarity among the tetranickel(II) cores in the five compounds **1**–**5** is that the two nickel(II) ions in the so-called Ni^{II}_2 fragment are bridged by a $\mu_{1,3}$-carboxylato ligand, which is *o*-benzoylbenzoato for **1**, **4** and **5**, phenyl acetato for **2** and salicylato for **3**. Clearly, there are two such carboxylatos in each of the Ni^{II}_4 compounds **1**–**5**. It is also obvious that, in **1**–**5**, one coordination position of each Ni^{II} center is occupied by an oxygen atom of a $\mu_{1,3}$-carboxylato ligand. In sharp contrast, there is no $\mu_{1,3}$-carboxylato ligand in **6**. Rather, there are one water and one monodentate azido ligands per Ni^{II}_2 fragment in **6**; one nickel(II) is coordinated to the azido nitrogen atom while the second is coordinated to the water oxygen atom. Obviously, the two metal ions in each Ni^{II}_2 fragment in **1**–**5** are bridged by a μ-phenoxo oxygen atom, a μ_3-methoxo/hydroxo/$\mu_{1,1,1}$-azido oxygen/nitrogen atom and a $\mu_{1,3}$-carboxylato oxygen atom, whereas the two metal ions in each Ni^{II}_2 fragment in **6** are bridged by a μ-phenoxo oxygen atom and a μ_3-/$\mu_{1,1,1}$-azido nitrogen atom.

For the sake of simplicity, it is logical not to discuss the structural parameters involving the ligand having minor occupancy in the μ_3-mixed-ligand. Each Ni^{II} center in **1**–**6** is hexacoordinated. The selected bond distances and angles involving Ni1 and Ni2 centers are listed in Tables S2, S3, S4 and S5. The ranges of bond distances involving the Ni1 centers in

1–**6** are, respectively, 1.994–2.166 Å, 2.012–2.148 Å, 1.997–2.146 Å, 2.012–2.174 Å, 1.994–2.185 Å and 1.989–2.114 Å, i. e., the differences between the longest and shortest bond distances are, respectively, 0.172 Å, 0.136 Å, 0.149 Å, 0.162 Å, 0.191 Å and 0.125 Å. The ranges of bond distances involving the Ni2 centers in **1**–**6** are, respectively, 2.028–2.084 Å, 2.038–2.073 Å, 2.044–2.074 Å, 2.029–2.090 Å, 2.001–2.134 Å and 2.029–2.172 Å, i. e., the differences between the longest and shortest bond distances are, respectively, 0.056 Å, 0.035 Å, 0.03 Å, 0.061 Å, 0.133 Å and 0.143 Å. Hence, the range of bond distances around Ni1 is wider in most cases. The bond distances involving the phenoxo oxygen atom (overall range: 1.994–2.032 Å) and imine nitrogen atom (overall range: 1.989–2.012 Å) for the Ni1 centers in **1**–**6** and the bond distances involving μ_3-methoxo/hydroxo oxygen atom (overall range: 2.022–2.034 Å) for the Ni1 centers in **1**–**4** are significantly shorter than the other bond distances (overall range: 2.063–2.174 Å) involving Ni1. However, even such a broad order is not found for the bond distances involving the Ni2 centers in **1**–**6**. The ranges of the deviations of the *transoid* angles from 180º are 1.44–14.74º and 5.72–11.10º for the Ni1 and Ni2 centers, respectively, and the ranges of the deviations of the *cisoid* angles from 90º are 10.94–14.23º and 10.20–11.69º for the Ni1 and Ni2 centers, respectively. This way, the bond distances and bond angles indicate that the coordination geometry for both Ni1 and Ni2 centers is distorted octahedral, slightly more distorted for the Ni1 centers. The results of SHAPE[15] analyses (Table S6) also support this assignment, according to which the 'best ideal' geometry is octahedral where the ranges of the deviations from the ideal geometry for Ni1 and Ni2 centers are 0.765–1.087 and 0.517–0.700, respectively.

It has been possible to analyze the supramolecular interactions in four (**1**, **4**, **5** and **6**) of the six compounds while it is logical not to comment anything about supramolecular interactions in the remaining two compounds (**2** and **3**) because the sites of interactions in the latter two cases are disordered. The compounds **1**, **4**, **5** and **6** exhibit H-bonding interactions (Table S7). In case of complexes **1**, **4** and **5**, one of the participating atom in intermolecular H-bonding is benzoyl oxygen atom (O7D) of the carboxylato moiety of one molecule. The other interacting counterparts are (i) alcohol moiety (O3–H3A) of the Schiff base ligand $[HL^1]^-$ for complex **1**; (ii) imine moiety (C7–H7) of $[HL^1]^-$ for complex **4** and (iii) aldehyde moiety (C8–H8) of $[HL^1]^-$ for **5**. Thus, complex **1** adopts a 1D topology (Figure 3), complex **4** adopts a 2D topology (Figure 4) and complex **5** forms a 1D chain (Figure S3). Complex **6** exhibits both intramolecular and intermolecular type H-bondings which result in the formation of a 2D topology (Figure S4). Intramolecular H-bonding takes place between coordinated water ligand (O4–H4B) and N8 of terminal azido ligand while intermolecular

interaction takes place between methyl moiety (C13–H13B) of $[HL^1]^-$ of one molecule and N7D of $\mu_{1,1,1}$-azido ligand of another molecule.

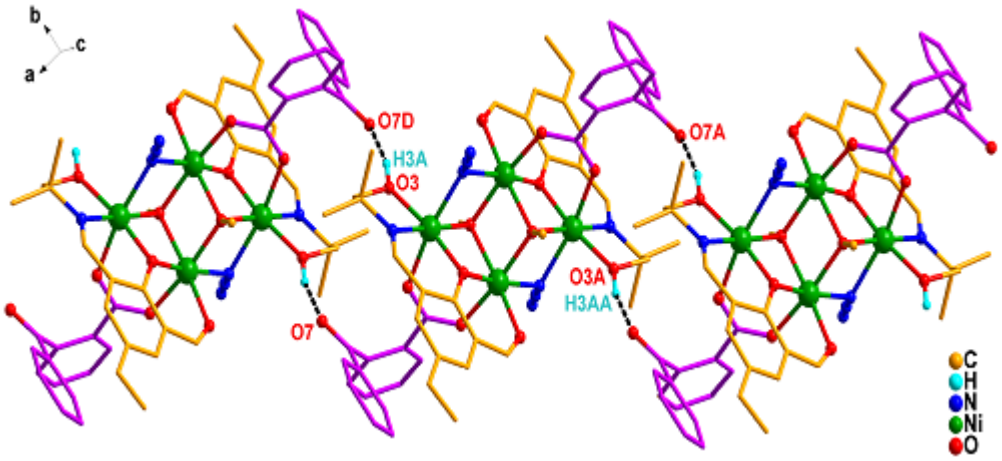

Figure 3. Intermolecular H–bonding mediated 1D supramolecular representation along the crystallographic *a* axis of $[Ni^{II}_4(HL^1)_2(\mu_3\text{-}OMe)_2(\mu_{1,1}\text{-}N_3)_2(\mu_{1,3}\text{-}o\text{-benzoylbenzoato})_2]$ (**1**). All hydrogen atoms except those participating in the H–bonding interactions have been omitted for clarity. Symmetry code: D = 0.5–x, 2.5–y, 1–z; A = –x, 2–y, 1–z.

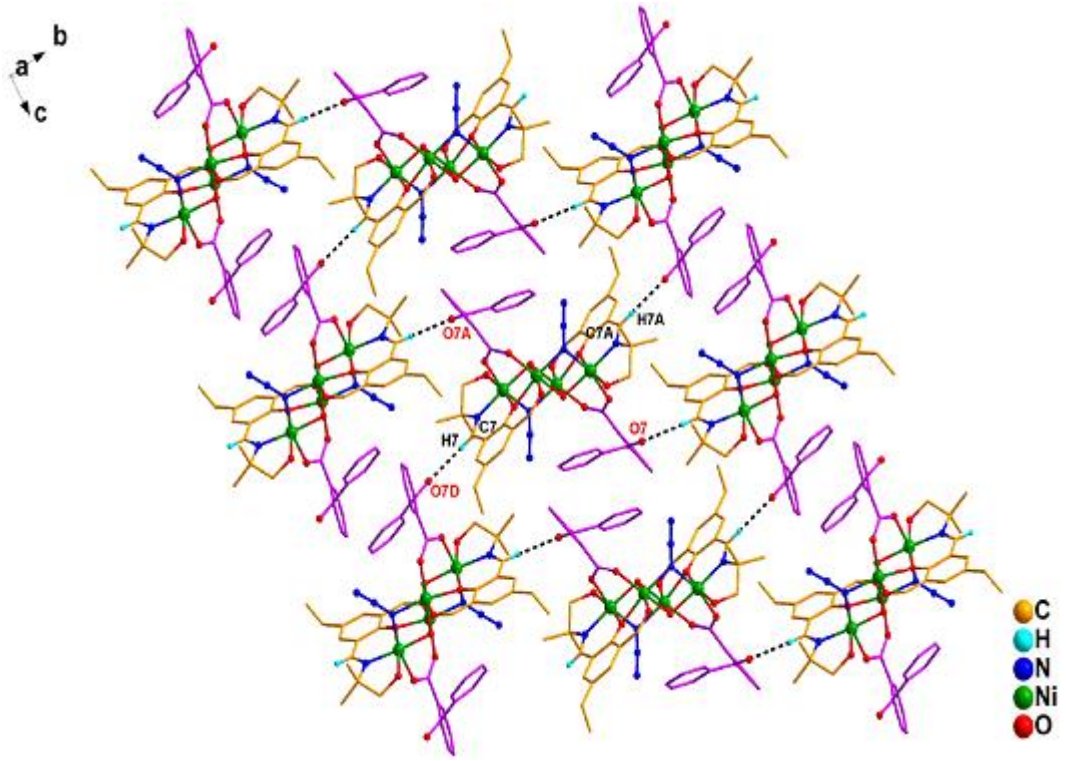

Figure 4. Intermolecular H–bonding mediated 2D supramolecular representation in the crystallographic *bc* plane of $[Ni^{II}_4(HL^1)_2(\mu_3\text{-}OH)_2(\mu_{1,1}\text{-}N_3)_2(\mu_{1,3}\text{-}o\text{-benzoylbenzoato})_2]\cdot 2H_2O$ (**4**). All hydrogen atoms except those participating in the H–bonding interactions have been omitted for clarity. Solvent of crystallisation molecules have also been omitted for simplicity. Symmetry code: D = 1–x, 0.5+y, 0.5–z; A = 1–x, 1–y, –z.

Magnetic Properties. DC magnetic susceptibility data (2–300 K) at 0.1 T field and magnetization data (up to 5 T) at 2, 4, 6, 8 and 10 K of **1**–**6** are shown in Figure 5 and S5, respectively. The $\chi_M T$ value at 300 K for **1**–**6** are, respectively, 5.77, 5.97, 5.81, 5.51, 5.95 and 5.07 cm^3 K mol^{-1}, which are greater than the theoretical value of 4.00 cm^3 K mol^{-1} (g = 2)/4.84 cm^3 K mol^{-1} (g = 2.2) for four noninteracting metal ions with $S_1 = S_2 = S_3 = S_4 = 1$. The variable-temperature profiles of the six compounds are similar. On lowering of temperatures from 300 K, the $\chi_M T$ value increases gradually to reach a maximum value (*ca*. 11.87, 11.13, 11.48, 11.37, 10.87 and 6.81 cm^3 K mol^{-1} for **1**–**6**, respectively) in a particular temperature range (*ca*. 10 K for **2**, **3, 4** and **6**, *ca*. 12 K for **1** and *ca*. 16 K for **5**) and then decreases rapidly to 8.48, 7.97, 9.62, 9.20, 6.99 and 5.43 for cm^3 K mol^{-1}, respectively, at 2 K. The profiles indicate the following: (i) Overall interaction in each of the six compounds is ferromagnetic; (ii) Rapid decrease in $\chi_M T$ at low temperatures takes place due to single-ion zero-field effect of Ni^{II}. The magnetization (M) data of all the six compounds up to 5 T at 2, 4, 6, 8 and 10 K were collected and are shown in Figure S5. The M values does not get saturated at 5 T and the values at 5 T and 2 K (7.08, 7.33, 7.72, 7.88, 7.07 and 7.54 Nβ, respectively) are lower than the theoretical value of 8.8 Nβ (g = 2.2) expected for S_T = 4. Hence, M versus H data also indicate the existence of zero-field effects. Therefore, magnetic properties of **1**–**6** should be modelled on taking into consideration of both exchange interactions and single-ion zero-field effects.

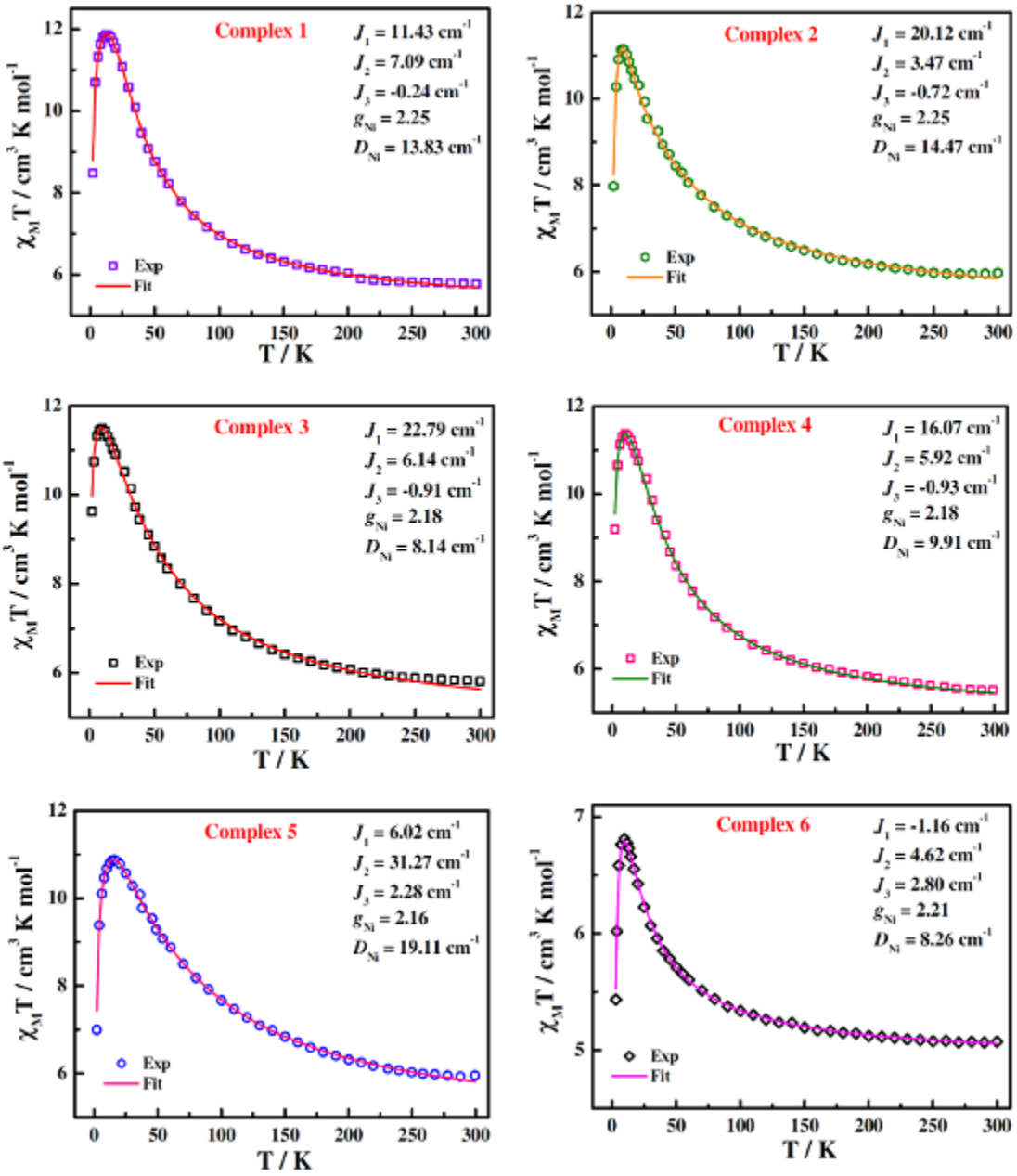

Figure 5. $\chi_M T$ versus T data of $[Ni^{II}_4(HL^1)_2(\mu_3\text{-OMe})_2(\mu_{1,1}\text{-}N_3)_2(\mu_{1,3}\text{-}o\text{-benzoylbenzoato})_2]$ (**1**) (Top left), $[Ni^{II}_4(HL^1)_2\{(\mu_3\text{-OMe})_{0.83}(\mu_3\text{-}N_3)_{0.17}\}_2(\mu_{1,1}\text{-}N_3)_2(\mu_{1,3}\text{-phenyl acetato})_2]\cdot 2H_2O$ (**2**) (Top right), $[Ni^{II}_4(HL^1)_2\{(\mu_3\text{-OMe})_{0.80}(\mu_3\text{-}N_3)_{0.20}\}_2(\mu_{1,1}\text{-}N_3)_2(\mu_{1,3}\text{-salicylato})_2]$ (**3**) (Middle left), $[Ni^{II}_4(HL^1)_2(\mu_3\text{-OH})_2(\mu_{1,1}\text{-}N_3)_2(\mu_{1,3}\text{-}o\text{-benzoylbenzoato})_2]\cdot 2H_2O$ (**4**) (Middle right), $[Ni^{II}_4(HL^1)_2\{(\mu_3\text{-}N_3)_{0.58}(\mu_3\text{-OMe})_{0.42}\}_2(\mu_{1,1}\text{-}N_3)_2(\mu_{1,3}\text{-}o\text{-benzoylbenzoato})_2]\cdot 2H_2O$ (**5**) (Bottom left) and $[Ni^{II}_4(HL^1)_2(\mu_{1,1,1}\text{-}N_3)_2(\mu_{1,1}\text{-}N_3)_2(N_3)_2(OH_2)_2]\cdot 4DMF$ (**6**) (Bottom right) between 2 and 300 K. The symbols are experimental data, while the solid lines represent the calculated curves.

In principle, there are three exchange integrals in each of **1**–**6** and these are as follows (Scheme 4): J_1, J_2 and J_3. J_1 is the integral between the two metal ions (Ni1 and Ni2 or Ni1A and Ni2A in **1**–**6**) in each of the two symmetry related Ni^{II}_2 fragments, where the two

concerned metal ions are triple-bridged in **1**–**5** and doubly-bridged in **6** by the following moieties: (i) One μ-phenoxo oxygen atom (for **1**–**6**); (ii) One μ_3-methoxo oxygen atom (for **1**) or one μ_3-hydroxo oxygen atom (for **4**) or one μ_3-methoxo-azido mixed ligand set (for **2**, **3** and **5**) or one $\mu_{1,1,1}$-azido (for **6**); (iii) Two oxygen atoms of one $\mu_{1,3}$-carboxylato ligand (for **1**–**4**). J_2 is the integral between the two metal ions (Ni1 and Ni2A or Ni1A and Ni2 in **1**–**6**) in two symmetry related pairs of metal ions, where the two concerned metal ions are double-bridged by the following moieties: (i) One $\mu_{1,1,}$-azido nitrogen atom(for **1**–**6**); (ii) One μ_3-methoxo oxygen atom (for **1**) or one μ_3-hydroxo oxygen atom (for **4**) or one μ_3-methoxo-azido mixed ligand set (for **2**, **3** and **5**) or one $\mu_{1,1,1}$-azido (for **6**). J_3 is the integral between two metal ions in only one pair (Ni2 and Ni2A), where the two concerned metal ions are bridged by bis(μ_3-methoxo) (for **1**) or bis(μ_3-hydroxo) (for **4**) or bis($\mu_{1,1,1}$-azido) (for **6**) or bis(μ_3-methoxo-$\mu_{1,1,1}$-azido mixed ligand set) (for **2**, **3** and **5**).

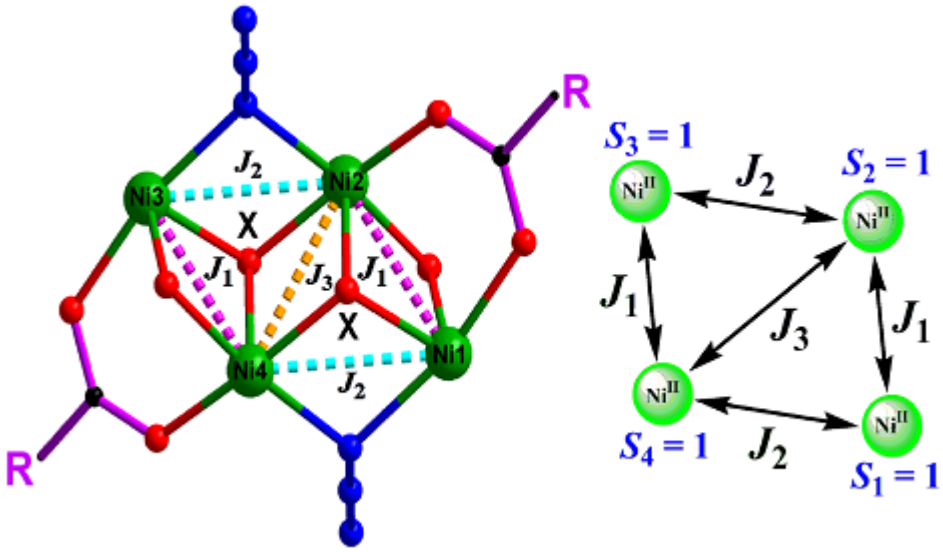

Scheme 4. Model for magnetic interactions in **1**–**6**. X = (OMe^-) for **1**, {$(OMe^-)_{0.83}(N_3^-)_{0.17}$} for **2**, {$(OMe^-)_{0.80}(N_3^-)_{0.20}$} for **3**, ($OH^-$) for **4**, {$(N_3^-)_{0.58}(OMe^-)_{0.42}$} for **5** and exclusively N_3^- for **6**. For **6**, $\mu_{1,3}$-RCO_2^- ligand is replaced by monodentate azido and water.

According to the above mentioned models of magnetic exchange interactions and taking into account the single-ion zero-field effect of Ni^{II} ions, the spin Hamiltonian for the magnetic properties of **1**–**6** can be given by

$$\mathbf{H} = -2J_1(\mathbf{S_1.S_2} + \mathbf{S_3.S_4}) - 2J_2(\mathbf{S_1.S_4} + \mathbf{S_2.S_3}) - 2J_3(\mathbf{S_2.S_4}) + D_{Ni}(\mathbf{S}_{1z}^2 + \mathbf{S}_{2z}^2 + \mathbf{S}_{3z}^2 + \mathbf{S}_{4z}^2)$$

Where $S_1 = S_2 = S_3 = S_4 = 1$. Using this general model Hamiltonian, the variable-temperature (2–300 K) susceptibility data under 0.1 T field and variable-field (up to 5 T) magnetization data at 2, 4, 6, 8, and 10 K were simultaneously simulated with the PHI program.[16] Good quality fittings were obtained (Figure 5, S5 and Table S8) with the following sets of converging parameters: J_1 = 11.43 cm^{-1}, J_2 = 7.09 cm^{-1}, J_3 = –0.24 cm^{-1}, D_{Ni} = 13.83 cm^{-1} and g = 2.25 for **1**; J_1 = 20.12 cm^{-1}, J_2 = 3.47 cm^{-1}, J_3 = –0.72 cm^{-1}, D_{Ni} = 14.47 cm^{-1} and g = 2.25 for **2**; J_1 = 22.79 cm^{-1}, J_2 = 6.14 cm^{-1}, J_3 = –0.91 cm^{-1}, D_{Ni} = 8.14 cm^{-1} and g = 2.18 for **3**; J_1 = 16.07 cm^{-1}, J_2 = 5.92 cm^{-1}, J_3 = –0.93 cm^{-1}, D_{Ni} = 9.91 cm^{-1} and g = 2.18 for **4**; J_1 = 6.02 cm^{-1}, J_2 = 31.27 cm^{-1}, J_3 = 2.28 cm^{-1}, D_{Ni} = 19.11 cm^{-1} and g = 2.16 for **5**; J_1 = –1.16 cm^{-1}, J_2 = 4.62 cm^{-1}, J_3 = 2.80 cm^{-1}, D_{Ni} = 8.26 cm^{-1} and g = 2.21 for **6**. Summary of static magnetic properties for all the compounds **1**–**6** has been given in Table S8. The D values in this series are positive and lie in the range from ~8 to ~19 cm^{-1}. It is worth mentioning that these D values are reliable because changing the magnitude or sign of D results in poor fitting of the susceptibility/magnetization data. However, the D values obtained here lie in the range of the reported examples and there are examples of higher D values of Ni^{II}.[6, 17] It may be mentioned that there is already a report in which different D values of some Ni^{II} compounds were listed.[17]

It is known that metal–O–metal and metal–N–metal bridge angles are the most important parameters in governing the nature and magnitude of magnetic exchange interactions propagated through, respectively, phenoxo/hydroxo/methoxo[1,2a–d] and $\mu_{1,1}$-azido[2e,f] bridges. Typically, the cross-over angle in phenoxo/hydroxo/methoxo bridged 3d-3d systems[1,2a–d] lie in the range 95–98º and the cross-over angle in diphenoxo-bridged dinickel(II) systems[2b] is 97.5º; the interaction is ferromagnetic if bridge angle is smaller than 97.5º and antiferromagnetic if bridge angle is greater than 97.5º. It is also a logical approximation that the latter specific correlation is also valid for hydroxo/methoxo-bridged systems. According to a DFT-computed correlation,[2e] the ferromagnetic interaction in $\mu_{1,1,}$-azido bridged dinickel(II) systems increases with the increase of Ni–N–Ni bridge angle and it becomes maximum when the bridge angle is 104º. It has been found experimentally also that the ferromagnetic interaction is negligible when Ni–N–Ni angle is close to 90º and the interaction increases as the bridge angle increases to *ca*. 105º.[2f] Notably, it is also a logical approximation that the correlations in $\mu_{1,1}$-azido systems can be valid to $\mu_{1,1,1}$-azido systems.

A model of exchange interactions of a system with four local spins can be represented by a rectangle. Such a rectangular representation of the exchange integrals in **1**–**6** is shown in Scheme 4, where J_1 corresponds to two opposite edges, J_2 corresponds to the two other

opposite edges and J_3 corresponds to a diagonal. Clearly, the value of J_3 is a unique solution in the simulations. On the other hand, as the four local spins are the same ($S_1 = S_2 = S_3 = S_4 = 1$), the simulated values of J_1 and J_2 are interchangeable, i. e., one of the two simulated values (for J_1 and J_2) of exchange integrals have to be assigned to J_1 and the second to J_2 on the basis of existing magneto-structural correlations. The task is not easy as the pathways of most magnetic interactions are heterobridged. Yet, as discussed below, the two simulated values can be logically well assignable to J_1 and J_2.

For the sake of simplicity, it is logical to omit the contribution of the ligand of minor occupancy of the μ_3-mixed-ligand set to assign J_1 and J_2. In the two Ni^{II}(μ-phenoxo-μ_3-methoxo/hydroxo-$\mu_{1,3}$-carboxylato)Ni^{II} pairs (J_1 route) in **1**–**4**, the ranges of Ni–O(phenoxo)–Ni and Ni–O(methoxo/hydroxo)–Ni angles are, respectively, 92.67–94.74º and 91.82–93.25º, and the average of the Ni–O–Ni angles in **1**–**4** are, respectively, 93.56º, 92.38º, 92.52º and 93.79º. These angles are smaller (by *ca*. 3.71–5.12º) than the cross-over angle (97.5º). Moreover there is countercomplementarity effect of $\mu_{1,3}$-carboxylato. Therefore, J_1 route should be ferromagnetic. In the two Ni^{II}(μ_3-methoxo/hydroxo-$\mu_{1,1}$-azido)Ni^{II} pairs (J_2 route) in **1**–**4**, the ranges of Ni–O(methoxo/hydroxo)–Ni and Ni–N($\mu_{1,1}$-azido)–Ni angles are, respectively, 101.15–103.35º and 96.62–97.15º, which should propagate moderate antiferromagnetic and moderate ferromagnetic interactions, respectively. Clearly, the J_2 routes should be less ferromagnetic than the J_1 routes in all of **1**–**4**. Therefore, of the two ferromagnetic J_1/J_2 values obtained in the simulations in each of **1**–**4**, the larger has been assigned to the J_1 route and the smaller to the J_2 route (J_1 = 11.43 cm^{-1} and J_2 = 7.09 cm^{-1} for **1**; J_1 = 20.12 cm^{-1} and J_2 = 3.47 cm^{-1} for **2**; J_1 = 22.79 cm^{-1} and J_2 = 6.14 cm^{-1} for **3**; J_1 = 16.07 cm^{-1} and J_2 = 5.92 cm^{-1} for **4**). In the two Ni^{II}(μ-phenoxo-$\mu_{1,1,1}$-azido)Ni^{II} pairs (J_1 route) in **6**, the Ni–O(phenoxo)–Ni and Ni–N($\mu_{1,1,1}$-azido)–Ni angles are, respectively, 100.40º and 93.70º, and hence they should propagate, respectively, weak antiferromagnetic and weak ferromagnetic interactions. Therefore, the J_1 route in this compound should be weakly ferromagnetic or weakly antiferromagnetic. In the two Ni^{II}($\mu_{1,1,1}$-azido-$\mu_{1,1}$-azido)Ni^{II} pairs (J_2 route) in **6**, the Ni–N($\mu_{1,1,1}$-azido)–Ni and Ni–N($\mu_{1,1}$-azido)–Ni angles are, respectively, 97.90º and 101.30º (i. e. closer to 104º than in the J_1 route (93.70º)) and hence the J_2 route in this compound should be more ferromagnetic than the J_1 route. Therefore, of the two J_1/J_2 values obtained in the simulations in **6**, the ferromagnetic value has been assigned to the J_2 route and the antiferromagnetic value to the J_1 route (J_1 = –1.16 cm^{-1} and J_2 = 4.62 cm^{-1}). In the two Ni^{II}(μ-phenoxo-$\mu_{1,1,1}$-azido-$\mu_{1,3}$-carboxylato)Ni^{II} pairs (J_1 route) in **5**, the Ni–O(phenoxo)–Ni and Ni–N($\mu_{1,1,1}$-azido)–Ni angles are, respectively, 95.19º and 91.23º

and hence both phenoxo and $\mu_{1,1,1}$-azido bridges in this compound should mediate only weakly ferromagnetic interactions; the interaction can be enhanced by the countercomplementarity effect of $\mu_{1,3}$-carboxylato. In the two $Ni^{II}(\mu_{1,1,1}$-azido-$\mu_{1,1}$-azido)Ni^{II} pairs (J_2 route) in **5**, the Ni–N($\mu_{1,1,1}$-azido)–Ni and Ni–N($\mu_{1,1}$-azido)–Ni angles are, respectively, 101.95º and 98.30º (both closer to 104º than in the J_1 route (91.23º)) and hence the J_2 route in this compound should be more ferromagnetic. Therefore, of the two ferromagnetic J_1/J_2 values obtained in the simulations in **5**, the larger has been assigned to the J_2 route and the smaller to the J_1 route (J_1 = 6.02 cm^{-1} and J_2 = 31.27 cm^{-1}).

The values of J_3 are small in each of **1**–**6**, from –0.24 to –0.93 cm^{-1} in **1**–**4**, 2.28 cm^{-1} in **5** and 2.80 cm^{-1} in **6**. In the $Ni^{II}(\mu_3$-methoxo/hydroxo-μ_3-methoxo/hydroxo)Ni^{II} pair (J_3 route) in **1**–**4**, the ranges of the average Ni–O(methoxo/hydroxo)–Ni angles are 97.37–98.88º, which are close to the value of cross-over angle, and therefore this route propagates only weak interaction. In the $Ni^{II}(\mu_{1,1,1}$-azido-$\mu_{1,1,1}$-azido)Ni^{II} pair (J_3 route) in **5** and **6**, the Ni–N–Ni angles are, respectively, 96.12º and 98.30º, which are significantly smaller than 104º. Therefore, weak ferromagnetic interactions are propagated through this type of route in **5** and **6**.

Comparison of 1–6 with related systems

Some structural and magnetic parameters of **1**–**6** and related known defect-dicubane compounds having similar bridging moieties are listed in Tables 1 and 2. Only a few defect-dicubane type Ni^{II}_4 compounds having core structures similar to those in **1**–**3**, **5** and **6** have been reported previously. It is worth mentioning that compounds **2**, **3** and **5** contain mixture of μ_3-methoxo and μ_3-azido core ligands between which former is the major μ_3-core ligand for **2** and **3** and latter is for **5**. Considering μ_3-methoxo as core ligand, there are six compounds similar to **1**–**3** and magnetic studies were done for five among those six (**I**–**V**).[4,5] On the other hand, considering μ_3-azido as core ligand there are one compound[6] (**VI**) similar to **5** and two compounds[6] (**VII** and **VIII**) similar to **6**. However, no related Ni^{II}_4 compound containing mixture of μ_3-methoxo and μ_3-azido core ligands has been reported previously. Again, there is no such Ni^{II}_4 compound with a μ_3-hydroxo core ligand (as in **4**) known. Hence, compounds **2**, **3**, **4** and **5** manifest a new type of μ_3-core bridging pattern with respect to structural view point.

Table 1. Relative comparison of Magnetic exchange coupling constant, ***J*** (cm^{-1}) values for defect dicubane like complexes exhibiting [Phenoxo, $\mu_{1,1,1}$-methoxo/hydroxo, $\mu_{1,3}$-carboxylato; $\mu_{1,1,1}$-methoxo/hydroxo, $\mu_{1,1}$-azido; Bis $\mu_{1,1,1}$-methoxo/hydroxo] type interactions in the tetranuclear Ni_4 core.

Compound	J_1 Route	Bridge Angles	Average Ni–O–Ni	J_1 Value	J_2 Route	Bridge Angles	J_2 Value	J_3 Route	Bridge Angles	Average Ni–O–Ni	J_3 Value	Ref.
1	μ-OPh μ_3-OMe $\mu_{1,3}$-RCO_2	94.74 92.38	93.56	11.43	μ_3-OMe $\mu_{1,1}$-N_3	102.17 96.62	7.09	μ_3-OMe μ_3-OMe	97.37 97.37	97.37	–0.24	This work
2	μ-OPh μ_3-OMe $\mu_{1,3}$-RCO_2	92.67 92.09	92.38	20.12	μ_3-OMe $\mu_{1,1}$-N_3	102.02 97.15	3.47	μ_3-OMe μ_3-OMe	98.25 98.25	98.25	–0.72	This work
3	μ-OPh μ_3-OMe $\mu_{1,3}$-RCO_2	93.22 91.82	92.52	22.79	μ_3-OMe $\mu_{1,1}$-N_3	101.15 96.95	6.14	μ_3-OMe μ_3-OMe	98.37 98.37	98.37	–0.91	This work
4	μ-OPh μ_3-OH $\mu_{1,3}$-RCO_2	94.33 93.25	93.79	16.07	μ_3-OH $\mu_{1,1}$-N_3	103.35 96.62	5.92	μ_3-OH μ_3-OH	98.88 98.88	98.88	–0.93	This work
I	μ-OPh μ_3-OMe $\mu_{1,3}$-RCO_2	93.80 92.30	93.05	13.75	μ_3-OMe $\mu_{1,1}$-N_3	102.90 97.20	10.31	μ_3-OMe μ_3-OMe	97.80 97.80	97.80	0.76	[4]
II	μ-OPh μ_3-OMe $\mu_{1,3}$-RCO_2	95.888 91.068	93.478	2.25	μ_3-OMe $\mu_{1,1}$-N_3	102.155 94.969	7.66	μ_3-OMe μ_3-OMe	98.36 98.36	98.36	≈J_1	[5a]
III	μ-OPh μ_3-OMe $\mu_{1,3}$-RCO_2	94.528 91.833	93.180	2.16	μ_3-OMe $\mu_{1,1}$-N_3	101.952 97.104	7.76	μ_3-OMe μ_3-OMe	99.392 99.392	99.392	≈J_1	
IV	μ-OPh μ_3-OMe $\mu_{1,3}$-RCO_2	94.864 92.484	93.674	2.34	μ_3-OMe $\mu_{1,1}$-N_3	102.010 97.189	8.93	μ_3-OMe μ_3-OMe	97.385 97.385	97.385	≈J_1	
V	μ-OPh μ_3-OMe $\mu_{1,3}$-RCO_2	95.10 91.10	93.10	5.80	μ_3-OMe $\mu_{1,1}$-N_3	102.30 97.90	14.75	μ_3-OMe μ_3-OMe	99.20 99.20	99.20	≈J_2	[5b]

Table 2. Relative comparison of Magnetic exchange coupling constant, ***J*** (cm^{-1}) values for defective dicubane like complexes exhibiting [Phenoxo, $\mu_{1,1,1}$-azido, ($\mu_{1,3}$-carboxylato); $\mu_{1,1,1}$-azido, $\mu_{1,1}$-azido; Bis $\mu_{1,1,1}$-azido] type interactions in the tetranuclear Ni_4 core.

Compound	***J*₁ Route**	**Bridge Angles**	***J*₁ Value**	***J*₂ Route**	**Bridge Angles**	**Average Ni–N–Ni**	***J*₂ Value**	***J*₃ Route**	**Bridge Angles**	**Average Ni–N–Ni**	***J*₃ Value**	**Ref.**
6	μ-OPh $\mu_{1,1,1}$-N_3 $\mu_{1,3}$-RCO_2	95.19 91.23	6.02	$\mu_{1,1,1}$-N_3 $\mu_{1,1}$-N_3	101.95 98.30	100.125	31.27	$\mu_{1,1,1}$-N_3 $\mu_{1,1,1}$-N_3	96.12 96.12	96.12	2.28	This work
VI	μ-OPh $\mu_{1,1,1}$-N_3 $\mu_{1,3}$-RCO_2	95.04 90.83	1.74	$\mu_{1,1,1}$-N_3 $\mu_{1,1}$-N_3	101.96 98.39	100.17	15.92	$\mu_{1,1,1}$-N_3 $\mu_{1,1,1}$-N_3	99.53 99.53	99.53	14.79	[6]
7	μ-OPh $\mu_{1,1,1}$-N_3	100.40 93.70	-1.16	$\mu_{1,1,1}$-N_3 $\mu_{1,1}$-N_3	97.90 101.30	99.60	4.62	$\mu_{1,1,1}$-N_3 $\mu_{1,1,1}$-N_3	98.30 98.30	98.30	2.80	This work
VII	μ-OPh $\mu_{1,1,1}$-N_3	100.70 94.35	-7.33	$\mu_{1,1,1}$-N_3 $\mu_{1,1}$-N_3	98.29 102.17	100.23	22.10	$\mu_{1,1,1}$-N_3 $\mu_{1,1,1}$-N_3	99.71 99.71	99.71	16.41	[6]
VIII	μ-OPh $\mu_{1,1,1}$-N_3	100.60 94.66	-5.59	$\mu_{1,1,1}$-N_3 $\mu_{1,1}$-N_3	99.15 100.25	99.70	17.96	$\mu_{1,1,1}$-N_3 $\mu_{1,1,1}$-N_3	98.60 98.60	98.60	16.71	

The primary ligands stabilizing the defective dicubane Ni^{II}_4 compounds are H_2L^1 and an analogous unsymmetrical ligand,[4] respectively, in **1**–**6** and **I**, H_3L type symmetrical ligands in **II**–**V**,[5] **VII**[6] and **VIII** [6] (Table S9). Clearly, **1**–**6** are the second examples of related defective dicubane Ni^{II}_4 compounds derived from H_2L^1 type of unsymmetrical ligands (the ligands having one O(alcohol)N(imine)O(phenol) and one O(aldehyde)O(phenol) compartments). The carboxylatos in **I**–**VI** are very similar; propionato in **I** and acetato in **II**–**VI**. On the other hand, different types of carboxylatos (*o*-benzoylbenzoato, phenylacetato and salicylato) are used in **1**–**6**. A H_3L type ligand[5a,6] (a (1:2) condensation product of 2,6-diformyl-4-methylphenol and 1-amino-2-propanol) is known to stabilize three defective dicubane type Ni^{II}_4 compounds, one[5a] ($[Ni_4(L^{III})_2(N_3)_2(CH_3COO)_2(CH_3O)_2]\cdot 2CH_3OH$, compound **III** in Table 1 and S9) with μ_3-methoxo and two $\mu_{1,3}$-carboxylatos, the second[6] ($[Ni_4(H_2L^{VI})_2(\mu\text{-}CH_3CO_2)_2(\mu_3\text{-}1,1,1\text{-}N_3)_2(\mu\text{-}1,1\text{-}N_3)_2]\cdot 2CH_3OH$, compound **VI** in Table 2 and S9) with $\mu_{1,1,1}$-azido and two $\mu_{1,3}$-carboxylatos and the third[6] ($[Ni_4(H_2L^{VII})_2(\mu_3\text{-}1,1,1\text{-}N_3)_2(\mu\text{-}1,1\text{-}N_3)_2(CH_3OH)_2Cl_2]\cdot 4CH_3OH$, compound **VII** in Table 2 and S9) with $\mu_{1,1,1}$-azido but having no carboxylatos, i. e. the concerned systems are similar to, respectively, **1**, **5** and **6**. However, stabilization of the following four types of systems derived from a single base ligand (H_2L^1) is unique : (i) System **1** having μ_3-methoxo and two $\mu_{1,3}$-carboxylatos; (ii) System **4** having μ_3-hydroxo and two $\mu_{1,3}$-carboxylatos; (iii) Systems **2**, **3** and **5** having mixture of μ_3-methoxo and $\mu_{1,1,1}$-azido and two $\mu_{1,3}$-carboxylatos; (iv) System **6** having $\mu_{1,1,1}$-azido but no carboxylato. Moreover, the solvent-dependent and both-way interconversions between the μ_3-methoxo compound **1** and μ_3-hydroxo compound **4** is interesting and in fact a new type of observation. In this context, it is worth mentioning that two defect-dicubane Ni^{II}_4 systems,[3f] $[Ni^{II}_4(\mu_3\text{-}OH)_2(H_2O)_6(ntp)_2]\cdot 2H_2O$ (**A**) and $[Ni^{II}_4(\mu_3\text{-}OMe)_2(H_2O)_6(ntp)_2$ (**B**), are produced in water and methanol, respectively ($H_3ntp = N(CH_2CH_2COOH)_3$). However, some reactants are different for the two compounds **A** and **B** ($NiSO_4\cdot 7H_2O$ and KOH for **A**; $NiCl_2$ and NaOH for **B**). Moreover, the interconversion between **A** and **B** was not reported.

Although the bridge angles are the most important governing parameters for magnetic properties, some other structural parameters including metal-ligand bond distances, metal···metal distances, dihedral angles in the bridging moieties, etc., along with the nature of Schiff base ligands and nature of carboxylatos, should influence the magnetic properties. Therefore, clear-cut relationship is difficult to achieve in **1**–**6** and **I**–**VIII** (Figure S6–S9). However, some qualitative relationship is observed. As in **1**–**6**, the overall interaction in all of **I**–**VIII** is ferromagnetic. Among **I**–**V**, three *J* values (J_1, J_2 and J_3) were considered only for

I. The order (magnitude) $J_1 > J_2 > J_3$ in **1**–**4** is same as that in **I**. J_3 values (0.76 cm^{-1} in **I**; from –0.93 to –0.24 cm^{-1} in **1**–**4**) are very small in **1**–**4** and **I**, which occurs because the bridge angle values in the J_3 route are close to the cross-over angle in these compounds. The bridge angles in both J_1 and J_2 routes in **I** are not very different from those in **1**–**4** and therefore the J_1 (13.75 cm^{-1} in **I** and 11.43–22.79 cm^{-1} in **1**–**4**) and J_2 values (10.31 cm^{-1} in **I** and 3.47–7.09 cm^{-1} in **1**–**4**) are comparable. As can be seen in Table 2, the bridge angle values in both J_1 route and J_2 route in **5** are slightly different from those in **VI** and both are ferromagnetic with the same order, $J_1 < J_2$ (J_1 = 6.02 cm^{-1} and J_2 = 31.27 cm^{-1} in **5**; J_1 = 1.74 cm^{-1} and J_2 =15.92 cm^{-1} in **VI**). The Ni–N–Ni bridge angles in the J_3 route in **5** and **VI** are 96º and 99º and both are ferromagnetic (J_3 = 2.28 cm^{-1} in **5** and 14.79 cm^{-1} in **VI**). The bridge angle values for the J_1 route in **6**, **VII** and **VIII** are close and, interestingly, this route is antiferromagnetic in these three compounds (J_1 = –1.16, –7.33 and –5.59 cm^{-1}, respectively).

Conclusions

The foci of this investigation have been the isolation of Ni^{II}_4 compounds with variable μ_3-core bridging ligands and studies of the magnetic properties of the derived systems. Six defective dicubane Ni^{II}_4 compounds (**1**–**6**) in this report contain a variable μ_3-core ligands (methoxo in **1**, hydroxo in **4**, $\mu_{1,1,1}$-azido in **6** and mixture of methoxo/$\mu_{1,1,1}$-azido in **2**, **3** and **5**). Moreover, to the best of our knowledge, regarding the mixed μ_3-core bridging ligands, three compounds in this investigation (**2**, **3** and **5**) are observed for the first time. An interesting and unique feature of this study is the solvent-dependent and both-way interconversion of a μ_3-methoxo and corresponding μ_3-hydroxo compounds (**1** and **4**, respectively).

The ligand, $[HL^1]^-$, herein is an unsymmetrical Schiff base moiety having one O(alcohol)N(imine)O(phenoxo) site and one O(aldehyde)O(phenoxo) site and, next to only one example,[4] **1**–**6** are the second examples of defective dicubane Ni^{II}_4 systems derived from such a base ligand. No other series is known where a particular base ligand stabilizes related systems with three different μ_3-core ligands (methoxo, hydroxo, $\mu_{1,1,1}$-azido). While only acetate in most cases and propionate in one case were used as the carboxylatos in related compounds, different types of carboxylatos (*o*-benzoylbenzoato, phenylacetato and salicylato) including some unusual acids have been used in this investigation.

Both variable-temperature and variable-field magnetic studies reveal overall ferromagnetic interactions in all of **1**–**6**. Both types of data have been simultaneously

simulated well with a three-*J* model and, interestingly, the exchangeable *J* values could be well assigned to the appropriate routes. Although the interactions are overall ferromagnetic, there are antiferromagnetic routes in some compounds. The results of **1**–**6** and previously reported compounds (only eight) follow some general trend.

Experimental Section

Caution! *Azido complexes of metal ions with organic ligands are potentially explosive. Only a small amount of material should be prepared, and it should be handled with care*.

Materials and physical measurements. All the reagents and solvents were purchased from commercial sources and used as received. 2,6-diformyl-4-ethylphenol was synthesized by a known procedure.[18] Elemental (C, H and N) analyses were performed on a Perkin-Elmer 2400 II analyzer. IR spectra were recorded in the region 400–4000 cm^{-1} on a Bruker-Optics Alpha–T spectrophotometer with samples as KBr disks. The magnetic measurements were carried out with a SQUID magnetometer (MPMS, Quantum Design). Diamagnetic corrections were taken into account based on Pascal's constants.

Syntheses.

H_3L solution. A solution of 2-amino-2-methyl-1-propanol (1.904 g, 20 mmol) in 25 mL methanol was added dropwise to a 35 mL methanol solution of 2,6-diformyl-4-ethylphenol (1.780 g, 10 mmol) under warming condition. The reaction mixture was refluxed for 3 h. After cooling, the volume of the solution was diluted to 100 mL in a volumetric flask. The resulting orange colored 'H_3L solution' was supposed to contain 10 mmol of the ligand H_3L and was utilised for subsequent reactions without further purification.

$[Ni^{II}_4(HL^1)_2(\mu_3\text{-}OMe)_2(\mu_{1,1}\text{-}N_3)_2(\mu_{1,3}\text{-}o\text{-benzoylbenzoato})_2]$ (1). To a 10 mL 'H_3L solution' containing 1 mmol H_3L was dropwise added under stirring a NaOH solution (0.120 g, 3 mmol) in minimum H_2O. The orange colored solution gradually turned into yellow. To it, 10 mL methanol solution of $Ni(ClO_4)_2{\cdot}6H_2O$ (0.731 g, 2 mmol) was added and the mixture was stirred for another 20 min. To the green colored clear solution, a solution of *o*-benzoyl benzoic acid (0.452 g, 2 mmol) in 10 mL methanol and a solution of sodium azide (0.130 g, 2 mmol) in minimum volume of water were successively added and the mixture was stirred for 2 h. The resulting yellowish green colored reaction mixture was filtered to remove any suspended particles and the filtrate was kept at ambient temperature for slow evaporation.

After few days, green colored crystalline compound containing diffraction quality single crystals were obtained, which was collected by filtration, washed with cold methanol and dried in vacuum.

Data for 1. Yield: 0.405 g (61%). Anal. calcd. For $C_{58}H_{60}N_8O_{14}Ni_4$ (FW: 1327.98): C, 52.46; H, 4.55; N, 8.44%. Found: C, 51.98; H, 4.64; N, 8.59%. Selected FT-IR data (cm^{-1}) on KBr: ν(N_3^-), 2063vs; ν(C=O), 1651vs; ν(C=N), 1633s; $\nu_{as}(COO^-)$, 1585m and $\nu_s(COO^-)$, 1390m.

$[Ni^{II}_4(HL^1)_2\{(\mu_3\text{-}OMe)_{0.83}(\mu_3\text{-}N_3)_{0.17}\}_2(\mu_{1,1}\text{-}N_3)_2(\mu_{1,3}$-phenyl acetato$)_2]\cdot 2H_2O$ (2) and $[Ni^{II}_4(HL^1)_2\{(\mu_3\text{-}OMe)_{0.80}(\mu_3\text{-}N_3)_{0.20}\}_2(\mu_{1,1}\text{-}N_3)_2(\mu_{1,3}$-salicylato$)_2]$ (3). These two compounds were prepared following the similar procedure as described for **1**, except that phenyl acetic acid (0.272 g, 2 mmol) and salicylic acid (0.276 g, 2 mmol) were used, respectively, for **2** and **3** instead of *o*-benzoylbenzoic acid.

Data for 2. Yield: 0.395 g (67%). Anal. calcd. For $C_{45.66}H_{58.97}N_{9.04}O_{13.65}Ni_4$ (FW: 1187.65): C, 46.17; H, 5.00; N, 10.66%. Found: C, 46.56; H, 4.90; N, 10.48%. Selected FT-IR data (cm^{-1}) on KBr: ν(O–H), 3443br; ν(N_3^-), 2113s and 2065vs; ν(C=O), 1651s; ν(C=N), 1633s; $\nu_{as}(COO^-)$, 1578m and $\nu_s(COO^-)$, 1380m.

Data for 3. Yield: 0.360 g (62%). Anal. calcd. For $C_{43.59}H_{50.79}N_{9.21}O_{13.6}Ni_4$ (FW: 1156.16): C, 45.28; H, 4.43; N, 11.16%. Found: C, 45.61; H, 4.49; N, 10.96%. Selected FT-IR data (cm^{-1}) on KBr: ν(N_3^-), 2069vs; ν(C=O), 1650vs; ν(C=N), 1633s; $\nu_{as}(COO^-)$, 1567m and $\nu_s(COO^-)$, 1405m.

$[Ni^{II}_4(HL^1)_2(\mu_3\text{-}OH)_2(\mu_{1,1}\text{-}N_3)_2(\mu_{1,3}$-*o*-benzoylbenzoato$)_2]\cdot 2H_2O$ (4). This complex was synthesized according to the similar procedure as that of **1**, except that 5 mL DMF was added to 10 mL 'H_3L solution' before the addition of an aqueous NaOH solution.

Data for 4. Yield: 0.394 g (59%). Anal. calcd. For $C_{56}H_{60}N_8O_{16}Ni_4$ (FW: 1335.92): C, 50.35; H, 4.53; N, 8.39%. Found: C, 50.14; H, 4.61; N, 8.55%. Selected FT-IR data (cm^{-1}) on KBr: ν(O–H), 3423br; ν(N_3^-), 2066vs; ν(C=O), 1647vs; ν(C=N), 1619s; $\nu_{as}(COO^-)$, 1557m and $\nu_s(COO^-)$, 1386m.

$[Ni^{II}_4(HL^1)_2\{(\mu_3\text{-}N_3)_{0.58}(\mu_3\text{-}OMe)_{0.42}\}_2(\mu_{1,1}\text{-}N_3)_2(\mu_{1,3}$-*o*-benzoylbenzoato$)_2]\cdot 2H_2O$ (5). This complex was prepared following the similar procedure as described for **1**, except that $Ni(ClO_4)_2\cdot 6H_2O$ (0.365 g, 1 mmol) and $MnCl_2\cdot 4H_2O$ (0.198 g, 1 mmol) were successively added instead of only $Ni(ClO_4)_2\cdot 6H_2O$ (0.731 g, 2 mmol).

Data for 5. Yield: 0.228 g (66%). Anal. calcd. For $C_{56.83}H_{60.49}N_{11.51}O_{14.83}Ni_4$ (FW: 1376.82): C, 49.57; H, 4.43; N, 11.71%. Found: C, 49.36; H, 4.29; N, 11.85 %. Selected FT-IR data

(cm^{-1}) on KBr: ν(O–H), 3461br; ν(N_3^-), 2092s and 2063vs; ν(C=O), 1650vs; ν(C=N), 1632vs; $\nu_{as}(COO^-)$, 1581m and $\nu_s(COO^-)$, 1391vs.

$[Ni^{II}_4(HL^1)_2(\mu_{1,1,1}\text{-}N_3)_2(\mu_{1,1}\text{-}N_3)_2(N_3)_2(OH_2)_2]\cdot 4DMF$ (6). To a 10 mL 'H_3L solution' containing 1 mmol H_3L was dropwise added under stirring a NaOH solution (0.120 g, 3 mmol) in minimum H_2O. The orange colored solution gradually turned into yellow. Then 10 mL methanol solution of $Ni(ClO_4)_2\cdot 6H_2O$ (0.731 g, 2 mmol) was added and stirred for another 20 min. To the resulting mixture, a solution of sodium azide (0.260 g, 4 mmol) in minimum volume of water was added and stirred. Immediately, a green solid started to deposit and the solution was allowed to stir for another 1 h. The solid was collected by filtration and washed with cold methanol. Recrystallization from a DMF–ether mixture (1:4) afforded a green crystalline compound containing diffraction quality single crystals.

Data for 6. Yield: 0.375 g (57%). Anal. calcd. For $C_{40}H_{68}N_{24}O_{12}Ni_4$ (FW: 1312.02): C, 36.62; H, 5.22; N, 25.62%. Found: C, 36.29; H, 5.14; N, 25.39%. Selected FT-IR data (cm^{-1}) on KBr: ν(O–H), 3451br; ν(N_3^-), 2107w, sh, 2079sh and 2056vs; ν(C=O), 1650vs; ν(C=N), 1631s.

Solvent dependent interconversion between 1 and 4/alternative way for synthesis of 1 and 4. Compound **4** (0.030 g, 0.02 mmol) was dissolved in MeOH (10 mL) under warming condition. The solution was taken in a long tube and ether was slowly added to make two separate layers. After a few days, crystals of **1** was formed which was collected by filtration and washed with cold methanol. Compound **1** (0.030 g, 0.02 mmol) was dissolved in DMF (10 mL) under warming condition. The solution was taken in a long tube and ether was slowly added to make two separate layers. After a few days, crystals of **4** was formed which was collected by filtration and washed with cold DMF-water (1:3) mixture.

Supporting Information: Contains Figures S1–S9, Tables S1–S9, crystal structure determination of **1**–**6** and CCDC number of **1**–**6**.

ACKNOWLEDGEMENTS

Financial support for this work has been received from Government of India through Council of Scientific and Industrial Research (fellowship to S. R.) and University Grants Commission (contingency from CAS-V project to S. M.). Crystallography was performed at the DST-FIST-funded Single Crystal Diffractometer Facility at the Department of Chemistry,

University of Calcutta. Center for Research in Nanoscience and Nanotechnology (CRNN), University of Calcutta, is acknowledged for magnetic studies.

Keywords: Magnetic Properties / Tetranickel(II) / Defect Dicubane / Ferromagnetic / Heterobridged.

References

[1] O. Kahn, *Molecular Magnetism*, VCH Publications, New York, **1993**.

[2] a) D. Venegas-Yazigi, D. Aravena, E. Spodine, E. Ruiz and S. Alvarez, *Coord*. *Chem*. *Rev*. **2010**, *254*, 2086–2095; b) K. K. Nanda, L. K. Thompson, J. N. Bridson and K. Nag, *Chem*. *Commun*. **1994**, 1337–1338; c) S. Sasmal, S. Roy, L. Carrella, A. Jana, E. Rentschler and S. Mohanta, *Eur*. *J*. *Inorg*. *Chem*. **2015**, 680–689; d) S. Ghosh, N. Hari and S. Mohanta, *ChemistrySelect* **2018**, *3*, 9402–9408; e) E. Ruiz, J. Cano, S. Alvarez and P. Alemany, *J. Am. Chem. Soc*. **1998**, *120*, 11122–11129; f) G. Manca, J. Cano and E. Ruiz, *Inorg*. *Chem*. **2009**, *48*, 3139–3144; g) S. K. Singh, N. K. Tibrewal and G. Rajaraman, *Dalton Trans*. **2011**, *40*, 10897–10906; h) T. Rajeshkumar and G. Rajaraman, *Chem*. *Comm*. **2012**, *48*, 7856–7858.

[3] a) S. Hazra, R. Koner, P. Lemoine, E. C. Sañudo and S. Mohanta, *Eur*. *J*. *Inorg*. *Chem*. **2009**, 3458–3466; b) P. S. Perlepe, A. A. Athanasopoulou, K. I. Alexopoulou, C. P. Raptopoulou, V. Psycharis, A. Escuer, S. P. Perlepes and T. C. Stamatatos, *Dalton Trans*. **2014**, *43*, 16605–16609; c) D. Das, G. Mahata, A. Adhikary, S. Konar and K. Biradha, *Cryst*. *Growth Des*. **2015**, *15*, 4132–4141; d) P.-P. Yang, C.-Y. Shao, Y. Xu and L.-L. Zhu, *Z. Anorg*. *Allg*. *Chem*. **2013**, *639*, 548–551; e) Z. Serna, N. D. la Pinta, M. K. Urtiaga, L. Lezama, G. Madariaga, J. M. Clemente-Juan, E. Coronado and R. Cortes, *Inorg*. *Chem*. **2010**, *49*, 11541–11549; f) P. King, R. Clérac, W. Wernsdorfer, C. E. Anson and A. K. Powell, *Dalton Trans*. **2004**, 2670–2676; g) T. N. Nguyen, K. A. Abboud and G. Christou, *Polyhedron* **2013**, *66*, 171–178; h) L. N. Dawe, T. S. M. Abedin, T. L. Kelly, L. K. Thompson, D. O. Miller, L. Zhao, C. Wilson, M. A. Leech and J. A. K. Howard, *J*. *Mater*. *Chem*., **2006**, *16*, 2645–2659; i) S. R. Parsons, L. K. Thompson, S. K. Dey, C. Wilson and J. A. K. Howard, *Inorg*. *Chem*. **2006**, *45*, 8832−8834.

[4] M. Pait, A. Bauzá, A. Frontera, E. Colacio and D. Ray, *Inorg*. *Chem*. **2015**, *54*, 4709–4723.

[5] a) S.-Y. Lin, G.-F. Xu, L. Zhao, Y.-N. Guo, J. Tang, Q.-L. Wang and G.-X. Liu, *Inorg. Chim. Acta* **2011**, *373*, 173–178; b) S. S. Tandon, S. D. Bunge, R. Rakosi, Z. Xu and L. K. Thompson, *Dalton Trans*. **2009**, 6536–6551; c) G. E. Kostakis, A. M. Ako and A. K. Powell, *Chem*. *Soc*. *Rev*. **2010**, *39*, 2238−2271; d) J. Ribas, A. Escuer, M. Monfort, R. Vicente, R. Cortés, L. Lezama and T. Rojo, *Coord*. *Chem*. *Rev*. **1999**, *193*, 1027−1068.

[6] S. S. Tandon, S. D. Bunge, N. Patel and J. Sanchiz, *Polyhedron* **2017**, *123*, 361–375.

[7] a) C. Wang, H. Du, X. Zhao, C. Jin, M. Tian, Y. Zhang and R. Che, *Nano Lett*. **2017**, *17*, 2921–2927; b) Y. Zeng, S.-J. Liu, C.-M. Liu, Y.-R. Xiea and Z.-Y. Du, *New J. Chem*. **2017**, *41*, 1212–1218; c) E.-Q. Gao, P.-P. Liu, Y.-Q. Wang, Q. Yue and Q.-L. Wang, *Chem. Eur. J*. **2009**, *15*, 1217–1226; d) C. Dendrinou-Samara, J. P. S. Walsh, C. A. Muryn, D. Collison, R. E. P. Winpenny and F. Tuna, *Eur. J. Inorg. Chem*. **2018**, 485–492; e) A. Karmakar, G. M. D. M. Rubio, M. F. C. Guedes da Silva, S. Hazra and A. J. L. Pombeiro, *Cryst. Growth Des*. **2015**, *15*, 4185−419.

[8] a) R. Sessoli, D. Gatteschi, A. Caneschi and M. A. Novak, *Nature* **1993**, *365*, 141–143; b) S. Mandal, S. Ghosh, D. Takahashi, G. Christou and S. Mohanta, *Eur. J. Inorg. Chem*. **2018**, 2793–2804; c) G. Aromí and E. K. Brechin, *Struct. Bonding* **2006**, *122*, 1–67; d) H.-R. Wen, P.-P. Dong, S.-J. Liu, J.-S. Liao, F.-Y. Lianga and C.-M. Liu, *Dalton Trans*. **2017**, *46*, 1153–1162; e) R. A. Layfield and M. Murugesu, *Lanthanides and Actinides in Molecular Magnetism*, Wiley-VCH, Weinheim, Germany 2015; f) S. Sanz, J. M. Frost, G. Lorusso, M. Evangelisti, M. B. Pitak, S. J. Coles, G. S. Nichol and E. K. Brechin, *Dalton Trans*., **2014**, *43*, 4622-4625.

[9] a) C. A. P. Goodwin, F. Ortu, D. Reta, N. F. Chilton and D. P. Mills, *Nature* **2017**, *548*, 439–442; b) S. G. McAdams, A.-M. Ariciu, A. K. Kostopoulos, J. P. S. Walsh and F. Tuna, *Coord. Chem. Rev*. **2017**, *346*, 216–239; c) A. Upadhyay, K. R. Vignesh, C. Das, S. K. Singh, G. Rajaraman and M. Shanmugam, *Inorg. Chem*. **2017**, *56*, 14260–14276; d) S. K. Gupta, T. Rajeshkumar, G. Rajaraman and R. Murugavel, *Chem. Sci*. **2016**, *7*, 5181–5191; e) S. Mandal, S. Mondal, C. Rajnák, J. Titiš, R. Boča and S. Mohanta, *Dalton Trans*. **2017**, *46*, 13135–13144.

[10] T. Ama, M. M. Rashid, T. Yonemura, H. Kawaguchi and T. Yasui, *Coord. Chem. Rev*. **2000**, *198*, 101–116.

[11] a) A. V. Funes, L. Carrella, Y. Rechkemmer, J. Van Slageren, E. Rentschler and P. Alborés, *Dalton Trans*. **2017**, *46*, 3400–3409; b) Y. Peng, V. Mereacre, C. E. Anson and A. K. Powell, *Dalton Trans*. **2017**, *46*, 5337–5343; c) K. Griffiths, C. W. D. Gallop, A. Abdul-Sada, A. Vargas, O. Navarro and G. E. Kostakis, *Chem. Eur. J*. **2015**, *21*, 6358–6361.

[12] a) A. Karmakar, P. Samanta, A. V. Desai and S. K. Ghosh, *Acc. Chem. Res*. **2017**, *50*, 2457–2469; b) Lotsch *et al*., *CrystEngComm*, **2013**, *15*, 9213 (Themed issue: Structural Design of Coordination Polymers); c) R.-P. Li, Q.-Y. Liu, Y.-L. Wang, C.-M. Liu and S.-J. Liu, *Inorg. Chem. Front*. **2017**, *4*, 1149–1156; d) D. G. Branzea, A. Guerri, O. Fabelo, C. Ruiz-Pérez, L.-M. Chamoreau, C. Sangregorio, A. Caneschi and M. Andruh, *Cryst. Growth Des*. **2008**, *8*, 941–949; e) S. Hazra, A. Karmakar, M. F. C. G. da Silva, L. Dlháň, R. Boča and A. J. L. Pombeiro, *New J. Chem*. **2015**, *39*, 3424–3434.

[13] a) S. S. Tandon, S. D. Bunge, D. Motry, J. Sanchez Costa, G. Aromi, J. Reedijk and L. K. Thompson, *Inorg. Chem*. **2009**, *48*, 4873–4881; b) S. Yamashita, T. Shiga, M. Kurashina, M. Nihei, H. Nojiri, H. Sawa, T. Kakiuchi and H. Oshio, *Inorg. Chem*. **2007**, *46*, 3810–3812; c) T. Shiga, N. Hoshino, M. Nakano, H. Nojiri and H. Oshio, *Inorg. Chim. Acta* **2008**, *361*, 4113–4117; d) T. Shiga and H. Oshio, *Polyhedron* **2011**, *30*, 3238–3241.

[14] a) K. Dhara, U. C. Saha, A. Dan, S. Sarkar, M. Manassero and P. Chattopadhyay, *Chem. Commun*. **2010**, *46*, 1754–1756; b) K. S. Banu, M. Mukherjee, A. Guha, S. Bhattacharya, E. Zangrando and D. Das, *Polyhedron* **2012**, *45*, 245–254.

[15] a) J. Cirera, E. Ruiz and S. Alvarez, *Chem. Eur. J*. **2006**, *12*, 3162–3167; b) M. Pinsk, and D. Avnir, *Inorg. Chem*. **1998**, *37*, 5575–5582.

[16] PHI Software. N. F. Chilton, R. P. Anderson, L. D. Turner, A. Soncini and K. S. Murray, *J. Comput. Chem*. **2013**, *34*, 1164–1175.

[17] S. Mandal, S. Majumder, S. Mondal and S. Mohanta, *Eur. J. Inorg. Chem*. **2018**, 4556–4565.

[18] a) F. Ullman and K. Brittner, *Chem. Ber*. **1909**, *42*, 2539–2548; b) S. Majumder, L. Mandal and S. Mohanta, *Inorg. Chem*. **2012**, *51*, 8739–8749; c) S. Majumder, S. Sarkar, S. Sasmal, E. Carolina Sanudo and S. Mohanta, *Inorg. Chem*. **2011**, *50*, 7540–7554.

Illustrated Synopsis

For

Syntheses, Crystal Structures and Magnetic Properties of a Series of Defect-Dicubane Tetranickel(II) Systems with Variable, Mixed and Interchangeable μ_3-Core Ligands

Shuvayan Roy, Hazel A. Sparkes and Sasankasekhar Mohanta*

Key Topic: Magnetic Properties of Clusters

This manuscript describes six defect-dicubane Ni^{II}_4 compounds containing two μ_3-methoxo or μ_3-hydroxo or μ_3-azido or mixture of μ_3-methoxo/μ_3-azido core ligands. Solvent-dependent and both-way interconversion between μ_3-methoxo and μ_3-hydroxo systems takes place. All exhibit overall ferromagnetic interactions.

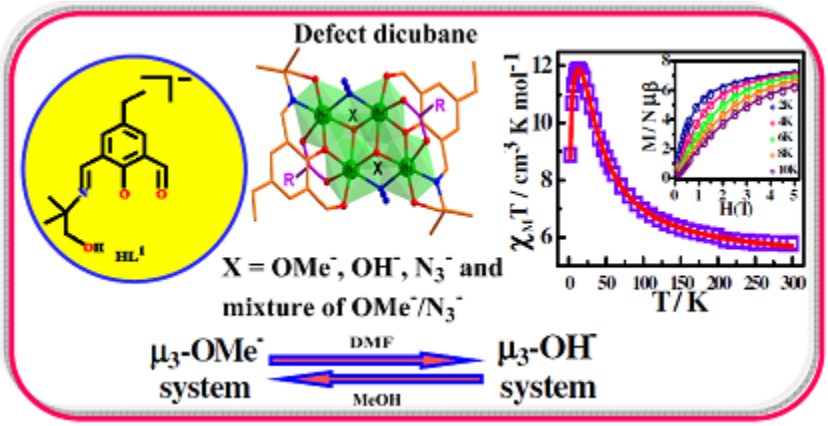

CIF

Checkcif

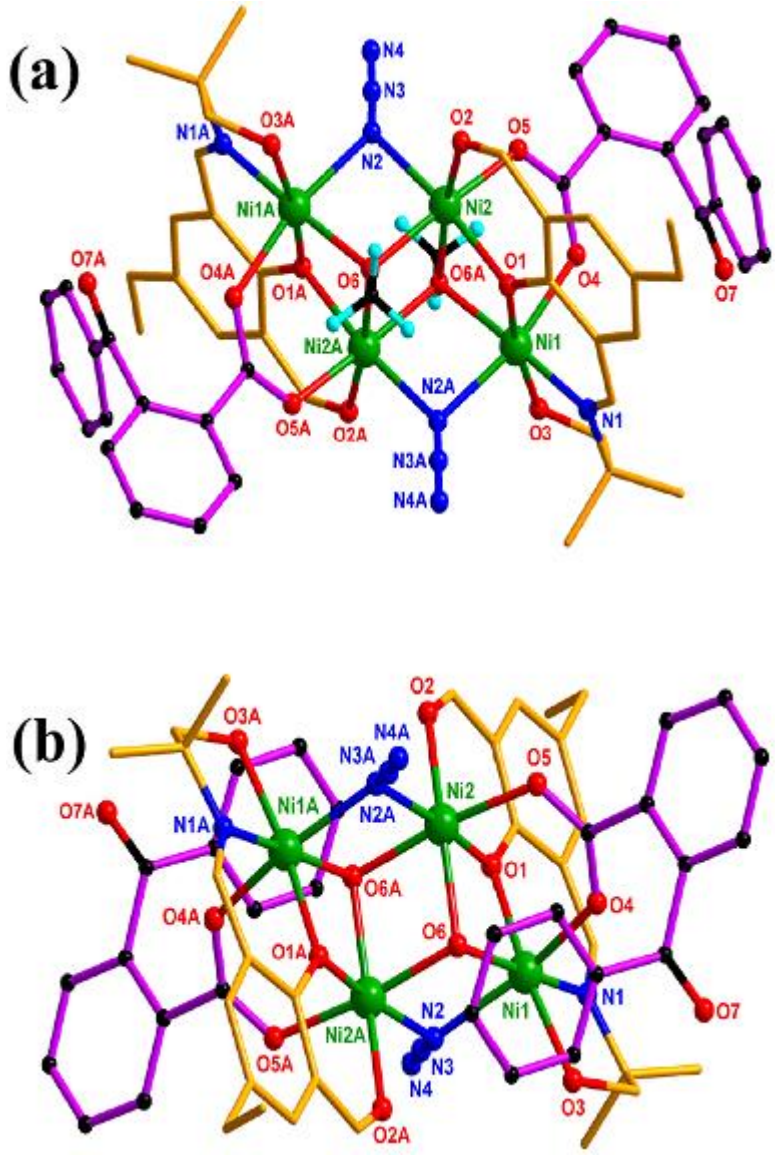

Figure 1. (a) Crystal structure of $[Ni^{II}_4(HL^1)_2(\mu_3\text{-}OMe)_2(\mu_{1,1}\text{-}N_3)_2(\mu_{1,3}\text{-}o\text{-benzoylbenzoato})_2]$ (**1**). All the hydrogen atoms except those of the core μ_3-methoxo bridging ligands have been omitted for clarity. Symmetry code: A = –x, 2–y, 1–z; (b) Crystal structure of $[Ni^{II}_4(HL^1)_2(\mu_3\text{-}OH)_2(\mu_{1,1}\text{-}N_3)_2(\mu_{1,3}\text{-}o\text{-benzoylbenzoato})_2]\cdot 2H_2O$ (**4**). Hydrogen atom on μ_3-hydroxo oxygen atoms (O6/O6A) were not inserted. All the other hydrogen atoms and water molecules of crystallization have been omitted for clarity. Symmetry code: A = 1–x, 1–y, –z.

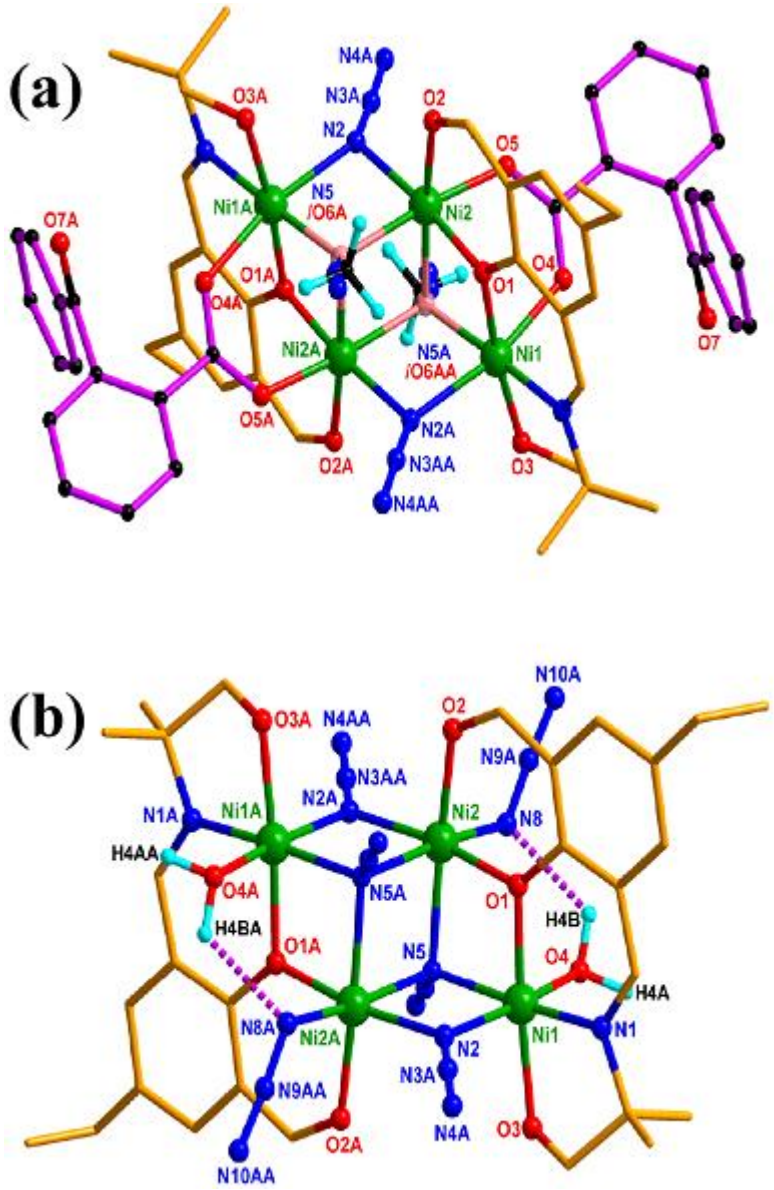

Figure 2. (a) Crystal structure of $[Ni^{II}_4(HL^1)_2\{(\mu_3\text{-}N_3)_{0.58}(\mu_3\text{-}OMe)_{0.42}\}_2(\mu_{1,1}\text{-}N_3)_2(\mu_{1,3}\text{-}o\text{-benzoylbenzoato})_2]\cdot 2H_2O$ (**5**). All the hydrogen atoms except those of the core μ_3-methoxo bridging ligands and two water molecules of crystallisation have been omitted for clarity. Symmetry code: A = 2–x, 1–y, 1–z; (b) Crystal structure of $[Ni^{II}_4(HL^1)_2(\mu_{1,1,1}\text{-}N_3)_2(\mu_{1,1}\text{-}N_3)_2(N_3)_2(OH_2)_2]\cdot 4DMF$ (**6**). All the hydrogen atoms except those of the coordinated water molecules have been omitted for clarity. Four DMF molecules of crystallisation have also been omitted for simplicity. Symmetry code: A = 1–x, 2–y, –z. The dotted lines represent intramolecular hydrogen bonding.

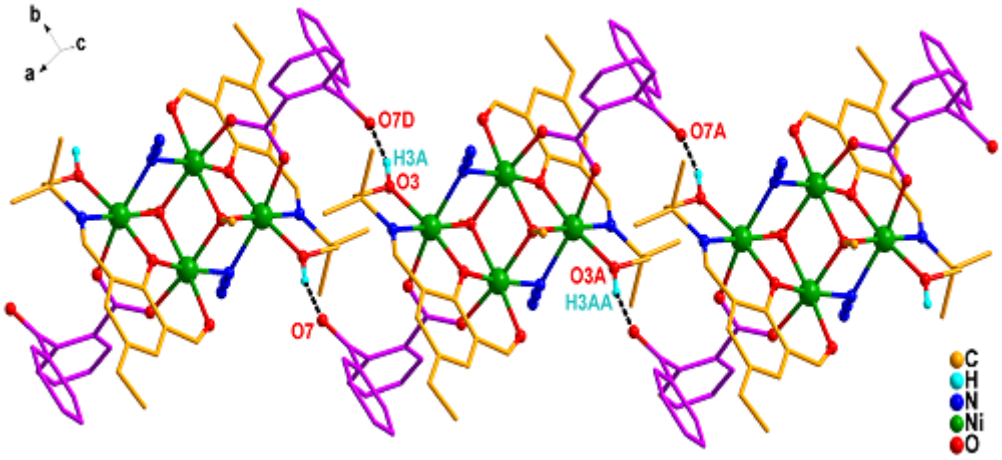

Figure 3. Intermolecular H–bonding mediated 1D supramolecular representation along the crystallographic *a* axis of $[Ni^{II}_4(HL^1)_2(\mu_3\text{-}OMe)_2(\mu_{1,1}\text{-}N_3)_2(\mu_{1,3}\text{-}o\text{-benzoylbenzoato})_2]$ (**1**). All hydrogen atoms except those participating in the H–bonding interactions have been omitted for clarity. Symmetry code: D = 0.5–x, 2.5–y, 1–z; A = –x, 2–y, 1–z.

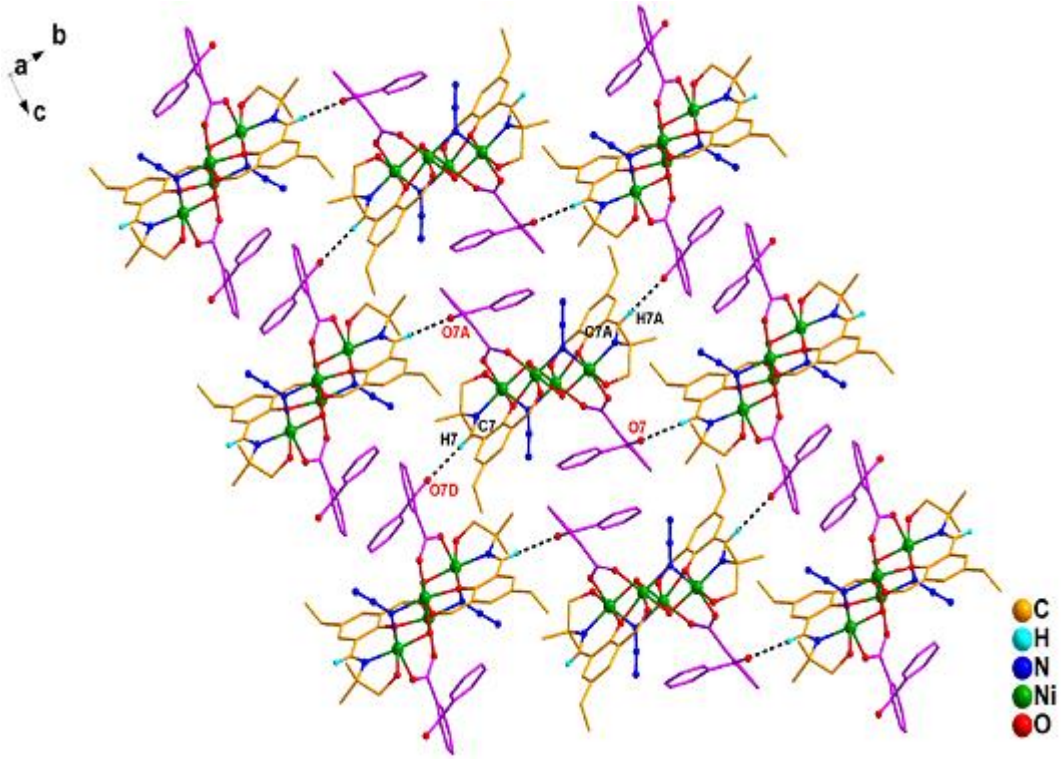

Figure 4. Intermolecular H–bonding mediated 2D supramolecular representation in the crystallographic *bc* plane of $[Ni^{II}_4(HL^1)_2(\mu_3\text{-}OH)_2(\mu_{1,1}\text{-}N_3)_2(\mu_{1,3}\text{-}o\text{-benzoylbenzoato})_2]\cdot 2H_2O$ (**4**). All hydrogen atoms except those participating in the H–bonding interactions have been omitted for clarity. Solvent of crystallisation molecules have also been omitted for simplicity. Symmetry code: D = 1–x, 0.5+y, 0.5–z; A = 1–x, 1–y, –z.

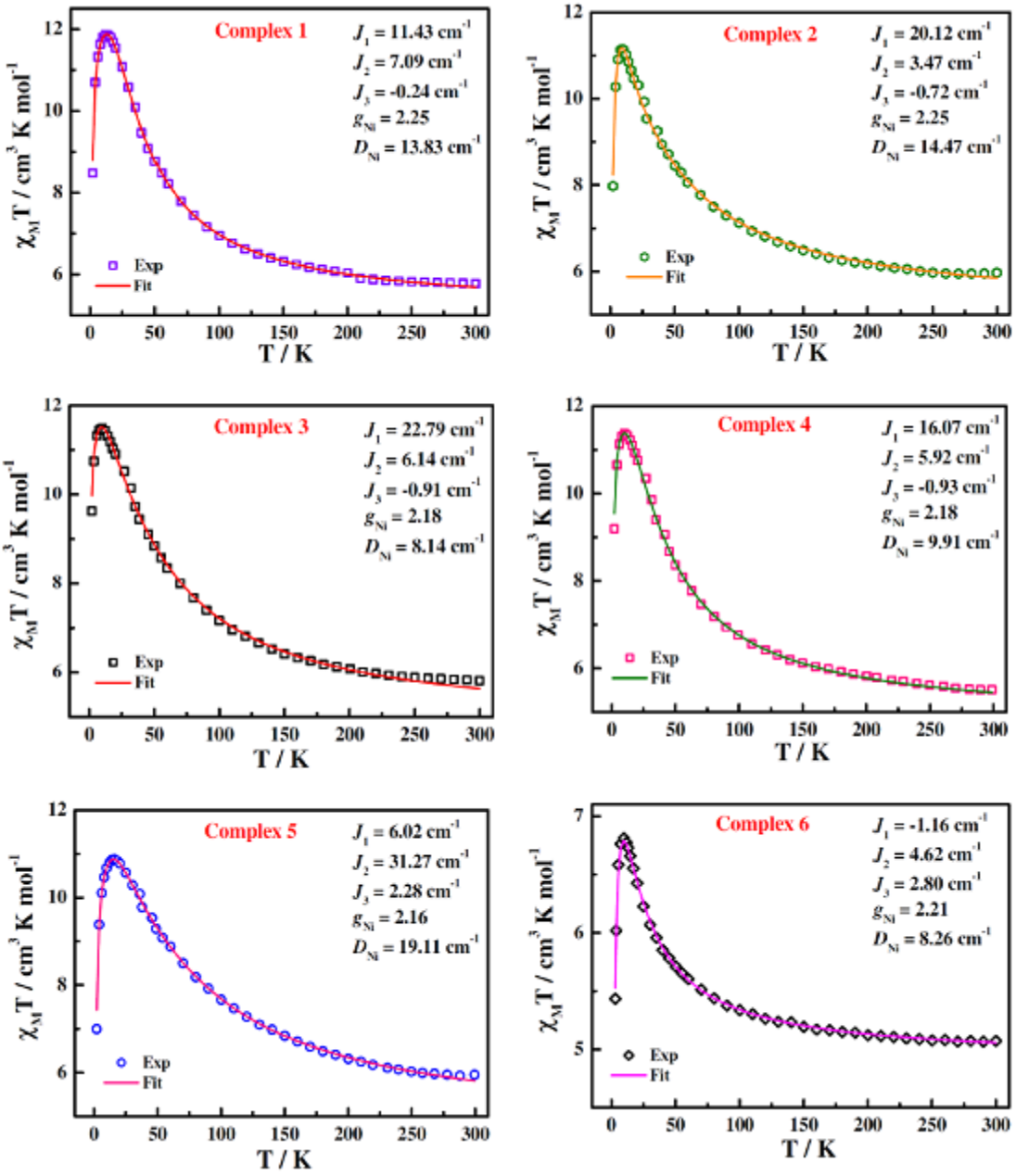

Figure 5. $\chi_M T$ versus T data of $[Ni^{II}_4(HL^1)_2(\mu_3\text{-OMe})_2(\mu_{1,1}\text{-N}_3)_2(\mu_{1,3}\text{-}o\text{-benzoylbenzoato})_2]$ (**1**) (Top left), $[Ni^{II}_4(HL^1)_2\{(\mu_3\text{-OMe})_{0.83}(\mu_3\text{-N}_3)_{0.17}\}_2(\mu_{1,1}\text{-N}_3)_2(\mu_{1,3}\text{-phenyl acetato})_2]\cdot 2H_2O$ (**2**) (Top right), $[Ni^{II}_4(HL^1)_2\{(\mu_3\text{-OMe})_{0.80}(\mu_3\text{-N}_3)_{0.20}\}_2(\mu_{1,1}\text{-N}_3)_2(\mu_{1,3}\text{-salicylato})_2]$ (**3**) (Middle left), $[Ni^{II}_4(HL^1)_2(\mu_3\text{-OH})_2(\mu_{1,1}\text{-N}_3)_2(\mu_{1,3}\text{-}o\text{-benzoylbenzoato})_2]\cdot 2H_2O$ (**4**) (Middle right), $[Ni^{II}_4(HL^1)_2\{(\mu_3\text{-N}_3)_{0.58}(\mu_3\text{-OMe})_{0.42}\}_2(\mu_{1,1}\text{-N}_3)_2(\mu_{1,3}\text{-}o\text{-benzoylbenzoato})_2]\cdot 2H_2O$ (**5**) (Bottom left) and $[Ni^{II}_4(HL^1)_2(\mu_{1,1,1}\text{-N}_3)_2(\mu_{1,1}\text{-N}_3)_2(N_3)_2(OH_2)_2]\cdot 4DMF$ (**6**) (Bottom right) between 2 and 300 K. The symbols are experimental data, while the solid lines represent the calculated curves.

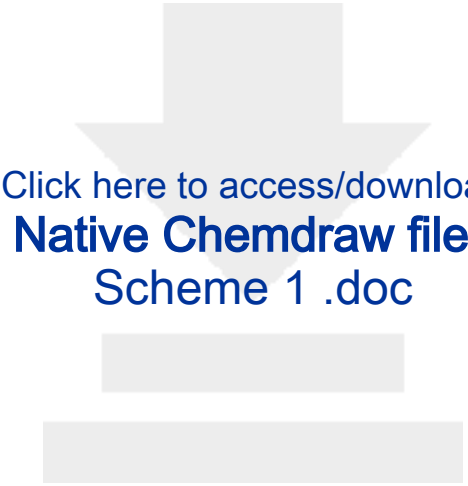

Click here to access/download

Native Chemdraw files

Scheme 1 .doc

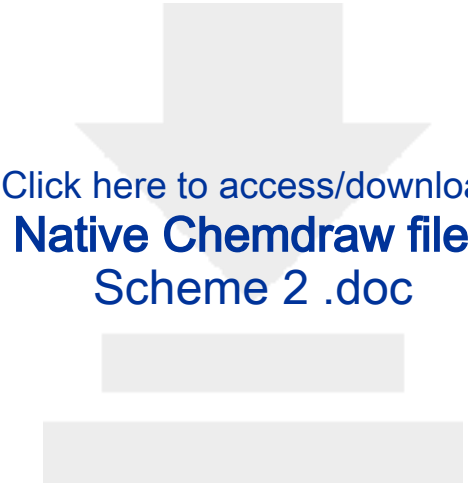

Click here to access/download

Native Chemdraw files

Scheme 2 .doc

Illustrated Synopsis

For

Syntheses, Crystal Structures and Magnetic Properties of a Series of Defect-Dicubane Tetranickel(II) Systems with Variable, Mixed and Interchangeable μ_3-Core Ligands

Shuvayan Roy, Hazel A. Sparkes and Sasankasekhar Mohanta*

Key Topic: Magnetic Properties of Clusters

This manuscript describes six defect-dicubane Ni^{II}_4 compounds containing two μ_3-methoxo or μ_3-hydroxo or μ_3-azido or mixture of μ_3-methoxo/μ_3-azido core ligands. Solvent-dependent and both-way interconversion between μ_3-methoxo and μ_3-hydroxo systems takes place. All exhibit overall ferromagnetic interactions.